ANL-4627
Chemistry

ARGONNE NATIONAL LABORATORY
P. O. Box 5207
Chicago 80, Illinois

Naval Reactor Division

ANALYSIS OF HEAT TRANSFER, BURNOUT, PRESSURE DROP AND DENSITY DATA FOR HIGH-PRESSURE WATER

by

W. H. Jens and P. A. Lottes

May 1, 1951

Operated by The University of Chicago
under
Contract W-31-109-eng-38

DISCLAIMER

Distribution	No. of Copies
Argonne National Laboratory	136
Armed Forces Special Weapons Project	1
Atomic Energy Commission, Washington	5
Battelle Memorial Institute	1
Brush Beryllium Company	1
Brookhaven National Laboratory	4
Bureau of Medicine and Surgery	1
Carbide and Carbon Chemicals Division (K-25 Plant)	4
Carbide and Carbon Chemicals Division (Y-12 Area)	4
Columbia University (G. Failla)	1
Dow Chemical Company	1
E. I. du Pont de Nemours and Company	5
General Electric, Richland	6
Idaho Operations Office	4
Iowa State College	2
Kellex Corporation	1
Knolls Atomic Power Laboratory	4
Los Alamos Scientific Laboratory	3
Mallinckrodt Chemical Works	1
Massachusetts Institute of Technology (A. Gaudin)	1
Massachusetts Institute of Technology (A. R. Kaufmann)	1
Mound Laboratory	3
National Advisory Committee for Aeronautics	1
National Bureau of Standards (R. D. Huntoon)	1
Naval Medical Research Institute	1
Naval Radiological Defense Laboratory	2
New Brunswick Laboratory	1
New York Operations Office	3
North American Aviation, Inc	1
Oak Ridge National Laboratory (X-10 Site)	8
Patent Branch, Washington	1
RAND Corporation	1
Sandia Corporation	1
Savannah River Operations Office	1
Sylvania Electric Products, Inc.	1
Technical Information Service, Oak Ridge	75
U. S. Geological Survey (T. B. Nolan)	2
U. S. Public Health Service	2
University of California at Los Angeles	1
University of California Radiation Laboratory	4
University of Rochester	2
University of Washington	1
Western Reserve University	1
Westinghouse Electric Corporation	2

Supplementary Distribution	No. of Copies
Atomic Energy Project, Chalk River	4
Chief of Naval Research	1
H. K. Ferguson Company	1
Harshaw Chemical Corporation	1
Isotopes Division (Mr. McCormick)	1
Library of Congress, Acquisition Department (J. W. Cormn)	2
National Bureau of Standards (Library)	1
National Research Council, Ottawa	1
Naval Research Laboratory	1
Nucleonics	1
Oak Ridge Institute of Nuclear Studies	2
United Kingdom Scientific Mission (M. Greenhill)	10
USAF, Eglin Air Force Base (Technical Library)	1
USAF, Wright-Patterson Air Force Base (Rodney Nudenberg)	1
USAF, Wright-Patterson Air Force Base (CADO)	5
U. S. Army, Army Medical Service Graduate School (Col. W. S. Stone)	1
U. S. Army, Atomic Energy Branch (Lt. Col. A. W. Betts)	1
U. S. Army, Technical Command (Col. J. H. Rothschild, Attn: Technical Library)	3
UT-AEC Agricultural Research Program (Charles S. Hobbs)	1
Total	342

TABLE OF CONTENTS

LIST OF FIGURES

LIST OF FIGURES

LIST OF FIGURES

LIST OF TABLES

ANALYSIS OF HEAT TRANSFER, BURNOUT, PRESSURE DROP AND DENSITY DATA FOR HIGH-PRESSURE WATER

ABSTRACT

Heat transfer, pressure drop, and water density data during forced convection and local boiling heat transfer have been correlated. These data were obtained by the University of California at Los Angeles, Massachusetts Institute of Technology, and Purdue University. All data were obtained on electrically heated tubes through which water passed in forced flow. From measurements of the attenuation of X-rays as they passed through the tube and the water, the density of the water was obtained under heat transfer conditions at UCLA.

In forced convection, the data correlated reasonably well with the Colburn equation. Dissolved gas had very little effect on the heat transfer coefficient.

The local boiling data were correlated by means of the following equation:

$$\Delta t_{sat} = \frac{60\left(\frac{q''}{10^6}\right)^{1/4}}{e^{\frac{P}{600}}}$$

The temperature of the heat transfer surface during boiling was independent of the water temperature and velocity and was dependent only on the heat flux and the water pressure. Dissolved gas had very little effect on the temperature of the heat transfer surface.

The heat flux that caused burnout was correlated as a function of water temperature, mass rate of flow, and pressure by means of the following type of equation.

$$\left(\frac{q''}{10^6}\right)_{B.O.} = C\left(\frac{G}{10^6}\right)^m \quad (t_{sat} - t_b)^{0.22}$$

The coefficient "C" and the exponent "m" were determined to be functions of water pressure.

The pressure drop during heat transfer with forced convection was reduced to existing correlations. The pressure drop during local and net boiling could not be correlated. The effect of dissolved gas and scale on pressure drop was unpredictable in most cases.

The density data obtained at high pressures using the X-ray measurements indicated that pressure has a very large effect on the density of water during local boiling.

ACKNOWLEDGEMENTS

The University of California research was conducted under a contract with the U. S. Atomic Energy Commission, Contract No. At-11-1-Gen-9. This research has been concluded and will be reported by UCLA. All of the data are on file with the Naval Reactor Division, Argonne National Laboratory, Chicago, Illinois

Massachusetts Institute of Technology research (DIC Project 6627) is being conducted under a contract with the Office of Naval Research, Contract No. N 5 ori-07827 and NR-035-267. This research is being reported in monthly progress reports. All of the data will be on file with the Naval Reactor Division, Argonne National Laboratory.

The Purdue University research was conducted on a contract with Argonne National Laboratory, Subcontract No. 31-109-38-212. The results of this research appear in the final summary report (Part I, ANL-4603). The Purdue University pressure drop and burnout data are on file with the Naval Reactor Division, Argonne National Laboratory.

The cooperation of Dean L. M. K. Boelter and his staff at UCLA, of Professor W. M. Rohsenow and his staff at MIT, and of Professor W. L. Sibbitt and his staff at Purdue with Argonne National Laboratory is appreciated.

I. NOMENCLATURE

A	Area, sq ft
C	Constant, dimensionless
C_p	Specific heat at constant pressure, Btu per lb per degree F
D	Diameter (inside) of tube, ft
f	Friction factor, dimensionless
f_c	Corrected friction factor, dimensionless
g	Conversion factor, ft per sec sq
G	Mass flow rate, lb per hr sq ft
h	Heat transfer coefficient, Btu per hr sq ft F
h_c	Heat transfer coefficient is given by the Colburn equation, Btu per hr sq ft F
k	Thermal conductivity of fluid, Btu per hr ft F
L	Heated length of tube, ft
M	Constant, dimensionless
N	Number of new bubbles of average size appearing on a unit surface per unit time, per sq ft sec

N_{Nu}	Nusselt number, dimensionless
N_{Pr}	Prandtl number, dimensionless
N_{Re}	Reynolds number, dimensionless
P	Pressure, lb per sq ft
q''	Heat flux, Btu per hr sq ft
q''_o	Heat flux at inception of boiling, Btu per hr sq ft
$q''_{B.O.}$	Heat flux at burnout, Btu per hr sq ft
R	Radius of vapor bubble, ft
R_{max}	Radius at full growth of the "average" vapor bubble at the conditions of heat transfer, ft
t	Time, sec
t_b	Bulk water temperature, F
t_{sat}	Saturation temperature, F
t_w	Heated wall temperature, F
v	Water velocity, fps
V	Volume, cu ft
V_b	Volume of vapor, cu ft
V_{mix}	Volume of mixture, cu ft
ΔP	Pressure drop, lb per sq ft
Δt_{sat}	Temperature difference between heated wall temperature and saturation temperature ($t_w - t_{sat}$), F
ΔT_{sub}	Temperature difference between saturation temperature and bulk water temperature ($t_{sat} - t_b$), F
$\Delta\rho$	Change in density, lb per cubic ft
δ	Percentage density change, dimensionless
ϵ	Roughness, ft
θ	Lifetime of an "average" bubble associated with heat transfer conditions, sec
μ	Viscosity, lb (mass) per ft hr
μ_b	Viscosity of water at bulk water temperature, lb (mass) per ft hr
μ_w	Viscosity of water at heated wall temperature, lb (mass) per ft hr
ρ	Density, lb per cu ft
ρ_ℓ	Density, of liquid, lb per cu ft
ρ_{mix}	Density of mixture of vapor and liquid, lb per cu ft
ρ_V	Density of vapor lb per cu ft

II INTRODUCTION

Heat transfer, burnout heat flux, pressure drop, and water density data for water at high pressures have been analyzed. These data have been collected at the University of California at Los Angeles, Massachusetts Institute of Technology, and Purdue University.

The systems used to collect the data at the three universities were basically the same. All incorporated a vertical tube of small diameter, electrically heated to produce high heat fluxes. Water under high total pressures was pumped upward through the tube.

A brief description of each system and the type of information secured are tabulated below.

EXPERIMENTAL SYSTEMS AT UCLA, MIT, AND PURDUE

Institution	UCLA	MIT	Purdue
Type of data	Heat transfer, burnout, pressure drop, density	Heat transfer, pressure drop	Heat transfer, burnout, pressure drop
Type of test section	Round tube, water inside	Round tube, water inside	Square and round tubes, water inside
Material of test section	Stainless steel type 347	Nickel	Stainless steel type 304
Diameter of test section	0.226 in. I.D.	0.18 in. I.D.	0.143 in. I.D.
Heated length	24.6 in.	9 in.	3 in. to 24 in.
Length-diameter ratio	108	50	21 to 168
Type of heating	Direct current	Direct current	Alternating current
Water condition	pH - 9.5	High resistivity maintained with ion exchanger	Treated boiler water
Gas addition to water	0 to 900 cc N_2/liter	None	None
Type of system	Closed	Closed	Open

All three institutions operated up to at least 2000 psia system pressure, 600F water temperature, 7,650,000 pounds per hr sq ft mass flow rate (40 fps at 400F), and 3,500,000 Btu per hr sq ft heat flux.

All tables and figures of data used in the analyses are included in Appendix A of this report.

III FORCED CONVECTION HEAT TRANSFER

UCLA has collected forced convection heat transfer data for pressures of 100 to 2000 psia, water temperatures of 229 to 636F, mass flow rates of 955,000 to 7, 650,000 pounds per hr sq ft, heat fluxes up to 2,000,000 Btu per hr sq ft, and additions of dissolved nitrogen up to 900 cc STP per liter of water at test conditions.

An analysis of early data from UCLA indicated a decrease in the apparent heat transfer coefficient and an increase of pressure drop with time Both of these phenomena were attributed to an increase of deposits or scale with time The deposits were mostly iron oxide. The use of an ion exchanger in the system did not appreciably retard or reduce scale at water temperatures greater than 400F. Later information with the pH of the water adjusted to a value greater than 9.5, by the addition of KOH showed no detectable change in the apparent heat transfer coefficient or pressure drop with time. Figure 1 (Appendix A) gives the results of tests which were run in order to demonstrate the effect of pH of the water on the formation of a deposit as it affected heat transfer and pressure drop. It was concluded that treated water greatly reduced and retarded the formation of scale.

Attempts to determine an L/D effect from the clean tube data were unsuccessful The UCLA data consistently showed a large heat transfer coefficient at the entrance of the heated tube, but a large exit coefficient was also indicated, with a minimum value near the middle of the tube. This observation can be verified by referring to Figure 2, which shows typical temperature and heat transfer coefficient variation along the heated tube.

The UCLA heat transfer data without pH control are shown in Figure 3 The tubes used in these runs were changed as soon as a noticeable decrease in the apparent heat transfer coefficient resulted. The data therefore can be expected to agree with the Colburn equation. For comparison purposes the data from a clean tube using water with a pH of 9.5 are shown in Figure 4. The scatter for the clean tube data is less than the scatter for the dirty tube data, but in both cases the data agree with the Colburn equation.

Dissolved nitrogen up to 900 cc per liter had no apparent effect on forced convection heat transfer at UCLA as indicated in Figure 4

MIT has collected forced convection heat transfer data at pressures of 1500 and 2000 psia, water temperatures of 320 to 600F, mass flow rates of 8000 to 5,740,000 pounds per hr sq ft (0.04 to 30 ft per sec), and heat fluxes up to 2,500,000 Btu per hr sq ft without dissolved gases.

MIT was able to reduce scale formation by using an ion exchanger in parallel with the pump A portion of the total water supply was circulated through the exchanger continuously. By this process water purity was main-

tained at a value less than 1 ppm of equivalent NaCl A typical plot of MIT data for both boiling and non-boiling conditions is shown in Figure 5. The effect on the temperature difference between the wall and the water with and without the ion exchanger is indicated.

MIT heat transfer data during forced convection at low velocities with the ion exchanger are shown in Figure 6 and compared with the Colburn equation. Data for all positions along the tube are plotted. The test points at Reynolds numbers of approximately 3000 and below lie in the transitional or laminar flow region.

Figures 7 through 11 are similar plots of data compared to the Colburn equation for larger Reynolds numbers. Each curve is for a different position along the tube. (The distance from the initial heating point divided by the diameter of the tube is defined as the position-diameter ratio.) The constant "C" in the heat transfer equation,

$$(N_{Nu}) = C\ (N_{Re})^{0.8}\ \ (N_{Pr})^{1/3}$$

is plotted as a function of these position-diameter ratios in Figure 12.

Purdue obtained forced convection heat transfer data for pressures of 250 to 1500 psia, water temperatures of 80 to 430 F, flow rates of 200,000 to 18,000,000 pounds per hr sq ft (1 to 90 fps), and heat fluxes up to 350,000 Btu per hr sq ft.

Figure 13 shows a comparison of some of the Purdue data with the Colburn equation. Considering the possibility of large amounts of scale on the heat transfer surface, the agreement with the Colburn equation is quite good.

A summary of the data from the three universities indicates:

(1) Scale of the type developed on nickel and stainless steel tubes could affect the heat transfer coefficient for forced convection, although it is not possible to isolate this effect from the data available. The thermal resistance of this scale had an equivalent coefficient of between 10,000 and 50,000 Btu per hr sq ft F, as can be deduced from the data in Figures 1 and 5.

(2) Dissolved nitrogen up to 900 cc per liter does not affect the heat transfer coefficient in forced convection, as indicated in Figure 4.

(3) The data at Reynolds numbers greater than 50,000 from clean heat transfer surfaces correlated with the Colburn equation to plus or minus 20 per cent. Data at lower Reynolds numbers and data obtained from scaled heat transfer surfaces correlate with the Colburn equation to plus or minus 50 per cent.

IV LOCAL BOILING HEAT TRANSFER

The local boiling data from UCLA and MIT cover pressures of 2500 to 85 psia, mass flow rates of 8000 to 7,650,000 pounds per hr sq ft, water temperatures of 300 to 600F, and heat fluxes to 2,500,000 Btu per hr sq ft.

These data may be plotted in different ways. The temperatures of the heated wall and water may be plotted as functions of position along the tube for the boiling runs similar to the non-boiling runs shown in Figure 2. Many plots of this type may then be further reduced by plotting the heat flux as a function of the temperature difference between the wall and water for various water temperatures at a constant flow rate and pressure as shown in Figures 5, 14, or 15. This type of plot is only of pictorial interest because actual data points are not shown in the boiling region. The data were represented more simply by determining Δt_{sat} as a function of heat flux and pressure as shown in Figures 16, 17, and 18; Δt_{sat} is defined as the heated surface temperature minus the saturation temperature.

The UCLA data at 500 psia were used to determine the effect of heat flux on Δt_{sat}. At 500 psia the values of Δt_{sat} varied between 14 and 33F; a scatter of plus or minus 5F did not obscure the effect of heat flux as a similar scatter did at pressures of 2000 psia where Δt_{sat} varied from 3 to 10F. In addition the heat flux was varied over a much greater range at 500 psia. The 500 psia data were plotted as shown in Figure 16. The slope of the curve was approximately 1/4 or very nearly the same as that used by McAdams, Addoms, and Kennel.[4] The McAdams local boiling data at 30, 60, and 90 psia for water flowing in an annulus were correlated by means of the following equation:

$$q'' = C\ \Delta t_{sat}^{3.86}$$

All UCLA data were reduced by dividing Δt_{sat} by the heat flux to the 1/4 power, and these values plotted as a function of pressure as shown in Figure 17. The data plotted were correlated to plus or minus 14F by means of the following equation:

$$\Delta t_{sat} = \frac{60\left(\frac{q''}{10^6}\right)^{1/4}}{e^{\frac{P}{900}}}$$

For comparison purposes the MIT data were replotted on the same basis as the UCLA data, as shown in Figure 18

In general it is felt that Δt_{sat} also depends on many other variables such as dissolved gas, adsorbed gas, condition and type of the heat transfer

surface, etc These variables could not be completely controlled and measured in this type of experiment It is significant, however, that the effects of these variables appear to be small

Table I in Appendix A gives the effect of dissolved gas on Δt_{sat} as measured at UCLA The effect is not predictable, but the variation is only a few degrees F In this connection, however, the point at which bubbling or boiling begins cannot be determined from the plot of Δt_{sat} as a function of heat flux or pressure. The type of curve used for this purpose is the pictorial curve of heat flux plotted vs wall temperature minus water temperature, at various water temperatures. The data in Figures 14 and 15 show two such curves with and without gas These curves are typical in that the point at which boiling begins is not appreciably affected by the introduction of gas. The last column in Table I presents observations of the point at which boiling begins In only a few instances was this point affected by the addition of gas.

V BURNOUT HEAT FLUX

UCLA and Purdue obtained burnout data for pressures from 500 to 2000 psia, water subcooling of 0 to 150F, mass rate of flow 960,000 to 7,500,000 lb per hr sq ft, and heat fluxes up to 4,000,000 Btu per hr sq ft without gas additions.

In order to establish a criterion for correlating the data a fictitious exit stream temperature, based on enthalpy rise, was used instead of measured outlet temperature. The actual exit stream temperatures with local boiling could not be calculated, since temperature gradients and distributions across a tube containing subcooled liquid and saturated vapor cannot be determined.

The UCLA data for burnout with subcooled water are shown in Table II. The Purdue data are shown in Table III.

For the UCLA data at pressures of 500, 1000, and 2000 psia three separate equations were found to correlate with the following equation:

$$\left(\frac{q''}{10^6}\right)_{B.O.} = C \left(\frac{G}{10^6}\right)^m (t_{sat} - t_b)^{0.22},$$

where

$(q'')_{B.O.}$ = burnout flux, Btu per hr sq ft

G = mass flow, lb per hr sq ft

t_{sat} = saturation temperature corresponding to flow conditions, F

t_b = water temperature at the position of burnout, F

C, m = constants, function of total pressure

The constant "m" was determined by the trend of all the data at a given pressure, while "C" was determined by the lower burnout heat flux. This was done in order to determine a correlation for a safe design.

The equation and data for 500 psia are shown in Figure 19, for 1000 psia in Figure 20, and for 2000 psia in Figure 21 Also shown are the final correlation for UCLA burnout data with subcooled water in Figure 22, the final correlation for Purdue burnout data with subcooled water based on the above general equation in Figure 23, and curves showing the dependency of "C" and "m" on total pressure for both UCLA and Purdue data in Figure 24.

Several items of significance are indicated by these data.

(1) The UCLA data correlated within 23 per cent for a wide range of variables. The Purdue data correlated within 60 per cent.

(2) With constant flow and constant subcooling, the burnout flux increases with a decrease in pressure between 2000 and 500 psia. This effect is pronounced at low velocities. No data were taken below 500 psia, so the effect at low pressures is not indicated

(3) There appears to be an L/D effect on the burnout heat flux. Purdue data are consistently higher than the UCLA data at all pressures Purdue tubes had an L/D ratio of 21, while UCLA tubes had an L/D ratio of 110.

Another correlation based on total temperature difference instead of subcooling might be possible The shape of the "C" vs pressure curves for UCLA and Purdue, Figure 24, resembles the shape of the curves representing the amount of wall superheat vs pressure during boiling, such as Figure 17. This type of correlation would be less useful than the present equation, since subcooling can be calculated more quickly and easily than total temperature differences between wall and water during local boiling

The UCLA data for burnout with net steam generation are listed in Table IV. The Purdue data for burnout with net steam generation are listed in Table V. There were not enough data points available to determine a satisfactory correlation.

Some of the test conditions with net steam generation showed unexpectedly high heat transfer rates Purdue, for example, demonstrated that a tube could be operated up to 3,000,000 Btu per hr sq ft at an inlet velocity

of 5 fps and a pressure of 280 psia. Calculations showed 31 per cent by weight net steam generation or 97 per cent steam by volume at the exit. UCLA has shown that a longer tube can be operated up to 1,890,000 Btu per hr sq ft heat flux at an inlet velocity of about 5 fps, pressure of 500 psia, and 50 per cent steam by volume at the exit.

VI. PRESSURE DROP AT HIGH WATER TEMPERATURES

The isothermal pressure drop data were obtained at water velocities ranging from 10 to 40 fps and water temperatures from 400 to 600F. The data covered various water conditions from neutral water (pH = 7) to treated water (pH = 9.5), with and without dissolved nitrogen.

In obtaining data at UCLA, approximately 40 tubes were used. Several of these tubes have been visually inspected, and the pressure drop data from these tubes were analyzed. The data from tubes 13 and 15 were analyzed since these tubes were used without pH control; however, these tubes were not available for inspection. Tubes 29, 30, and 39 were used with water pH of 9.5. Inspection of these tubes indicated that tube 29 was very clean, tube 30 had a black or dark brown coating that could be removed with an eraser, leaving a shiny surface, and tube 39 had a light straw color which was not effected by erasing.

Calculated isothermal friction factors are listed in Table VI. These friction factors are shown plotted vs. Reynolds number in Figure 25. The two curves appearing on the sheet where taken from Moody's friction factor curves (5), one for a smooth tube and the other for a tube with a roughness ratio of $\frac{\epsilon}{D} = 0.0002$. The roughness ratio of $\frac{\epsilon}{D} = 0.0002$ was chosen since it represents the isothermal friction factors for a smooth drawn tube of 0.226 inch I.D.

Several conclusions can be drawn from the isothermal pressure drop data.

(1) The nitrogen content of the water up to 900 cc per liter had very little effect on the isothermal friction factor as indicated in Table VI for tubes 30 and 39.

(2) The isothermal friction factor is affected to a slight degree by water temperature-higher water temperatures causing lower friction factors. Test points for the runs with water temperatures near 600F and Reynolds numbers near 17,000 fall on the curve for a theoretically smooth tube, while test points for all other runs (Tube 13 excluded) fall on the curve representing commercially drawn tubing.

The decrease of the isothermal friction factor with increased water temperature is not due to a change in tube diameter due to expansion. A change of tube temperature from 100F to 700F would decrease the friction factor due to a change in diameter by only 3 per cent, while the actual decrease in friction factor from tube temperatures of 400 to 600F was approximately 10 per cent for tube 39.

(3) The displacement of the data of tube 29 from the data of tube 39 could be due to a difference in inner diameter of the tubes. If the inside diameter of tube 29 were 2 per cent larger than the diameter of tube 39, the friction factor would be 10 per cent smaller since for a given weight rate of flow, the pressure drop varies approximately inversely as the fifth power of the diameter Typical tube dimensions show a variation of 1.6 per cent in inside diameter from one tube to another An accurate evaluation of the effect of tube dimensions will have to await the receipt of these dimensions.

(4) With neutral water (pH = 7), scale or deposits and pressure drop are unpredictable at water temperatures above 400F. The data from tube 13 indicated quite a variation in isothermal friction factor, compared to the data of tube 15.

(5) With pH control (pH = 9.5), a visible amount of dark coating had no effect on friction factor. The data from tubes 30 and 39 fell on a single curve corresponding to a commercially drawn tube. Actually, the data from the worst tube, 30, showed lower friction factors than from tube 39. This displacement, however, may be due to a difference in inner diameters of the two tubes as mentioned in item three above.

The general equation (3) for non-isothermal pressure drop for forced convection flow through a circular pipe is

$$P_1 - P_2 = \frac{fG^2}{2\rho_{ave}g}\left(\frac{L}{D}\right)\left(\frac{\mu_w}{\mu_b}\right)^{0.14} + \frac{G^2}{g}\left(\frac{1}{\rho_2} - \frac{1}{\rho_1}\right)$$

where

f = friction factor, dimensionless

G = mass flow rate, lb per sec sq ft

ρ = fluid density, lb per cu ft

g = conversion factor, ft per sec sq

L = length, ft

μ_w = viscosity at temperature of tube wall, lb (mass) per ft hr

μ_b = viscosity at fluid bulk temperature, lb (mass) per ft hr

P = pressure, lb per sq ft

D = diameter, ft

Purdue reported non-isothermal friction factors for water flowing through round and square tubes. The data covered a pressure range of 300 to 1500 psia, water temperatures of 70 to 550F, flow rates of 200,000 to 6,000,000 lb per hr sq ft (1 to 30 fps), and heat fluxes up to 800,000 Btu per hr sq ft.(6)

A comparison of the Purdue data with the Moody curve for a smooth tube is shown in Figure 26. Apparently the scale present in the Purdue system had little effect on the friction factor. The Purdue system used water treated with trisodium phosphate. This water was preheated in a Babcock and Wilcox forced flow boiler before entering the test section. Although tubes used in the tests showed brown deposits or films when split axially, the scale was less than 0 001 inch thick.

UCLA pressure drop data were taken along with heat transfer data. A typical pressure drop curve is shown in Figure 27 This curve shows three different flow conditions. From 0 to 356,000 Btu per hr sq ft heat input, the flow was forced convection. At a heat flux of 356,000 Btu per hr sq ft, the exit tube wall temperature was calculated to be 638F - the temperature at which boiling would start at the tube exit. This temperature was calculated using a value of heat transfer coefficient 20 per cent lower than the Colburn equation since this would give the lowest heat flux at which boiling would initiate. Between 357,000 and 528,000 Btu per hr sq ft, the flow was forced convection at the entrance with local boiling starting at some point along the tube. Beyond 528,000 Btu per hr sq ft, entire tube length was under fully developed local boiling. The calculated curve for frictional pressure drop was based on the average liquid density. The difference between the actual pressure drop and frictional pressure drop is in part due to the energy lost in accelerating the fluid from the inlet to the outlet of the tube.

The pressure drop curve did not break sharply at the point of incipient boiling at the tube exit, nor did a sharp break occur at the point of fully developed local boiling. The sharp increase occurred at a calculated exit subcooling of 8F.

In attempting to correlate the data, the experimental pressure drop curves were compared with calculated pressure drop curves; the points at which the experimental pressure drops began to deviate sharply from the calculated pressure drops were defined in terms of pressure, mass flow rate, inlet subcooling, calculated exit subcooling, and amounts of dissolved nitrogen. The rate of change of pressure drop was also indicated in terms of per cent pressure drop increase divided by per cent heat flux increase. Table VII shows the results of these calculations.

It is evident that the subcooling at which the break in the curves occurred for the first five sets of runs in Table VII was independent of the mass flow rate. A comparison of these runs with the next to last run in

Table VII shows an effect due to inlet subcooling or inlet water temperature. There are not enough data to determine definitely the effects of dissolved gases on pressure drop. However, certain trends are evident. Figures 28, 29, and 30 show a comparison between runs with the gas and without gas. In general, at 600F inlet water temperature, dissolved gas caused the break in the pressure drop curve to occur more gradually and at a lower heat flux. There is a discrepancy between the data of Figures 28 through 30 and the data of Figure 29. Figure 29 is for a mass flow rate of 5,730,000 lb per hr sq ft, a value less than that for Figure 30 and greater than that for Figure 28. With all other conditions constant, the curve with gas in Figure 29 shows little change from the curve without gas, while the curves in Figures 28 and 30 show as much as a 20 per cent change in heat input for the same pressure drop.

Figures 31 and 32 for 500F and 400F inlet water temperatures show the effect of gas to be negligible at these temperatures.

The pressure drop data at 2000 psia (Table VII) did not show an increase of

$$\frac{\frac{\Delta(\Delta P)}{\Delta P}}{\frac{\Delta q''}{q''}}$$

greater than 1 in the boiling region.

Except for the above limited observations, no definite conclusions were made or correlations found to describe pressure drop with heat input in the local boiling region.

Purdue reported pressure drop data for pressures of 1000 to 3000 psia, mass flow rates of 3,000,000 to 7,650,000 lb per hr sq ft, inlet water temperatures of 300 to 650F, and heat fluxes up to 3,650,000 Btu per hr sq ft for local boiling in a 0.143 in. I.D. x 3 in. long tube. In order to reduce scale formation with boiling, the power was on for only brief periods of time. A fifteen-second heating period was sufficient to reach steady state boiling and to collect data. For every set of test conditions, a run with zero heat input was made initially, followed by a run with local boiling, and terminated with a second zero heat input run. Figure 33 shows the results of these experiments. With few exceptions, within the limits of experimental accuracy, the friction factor did not change from the condition of isothermal flow to the condition of local boiling. The friction factors more nearly approached the Moody smooth tube line at high water temperatures, as was also shown in the UCLA data.

MIT collected pressure drop data for pressures of 1500 and 2000 psia, mass flow rates of 1,910,000 to 5,750,000 pounds per hr sq ft (10 to 30 fps), inlet water temperatures of 300 to 450F, and heat fluxes up to 3,000,000 Btu per hr sq ft. The data are listed in Table VIII. A comparison of the non-boiling friction factors with the Moody smooth tube is shown in Figure 34.

Sharp increases in pressure drop were noticed in the boiling regions. Since the inlet temperature varied considerably during a given set of runs, it is difficult to interpret the data in terms of subcoolings, flow rates, etc., where the sharp increase occurred.

VII DENSITY OF WATER AND WATER VAPOR MIXTURES DURING LOCAL BOILING

A formula was derived from the measurements by F. C. Gunther[2] in surface boiling of water with forced convection for atmospheric pressure, subcooling of 60 to 200F, velocity of 5 to 20 fps, and heat input of 726,000 to 3,370,000 Btu per hr sq ft.

$$\frac{\Delta\rho}{\rho} \times 100 = \frac{3 \times 10^8 \left(\frac{q''}{q''_o}\right)^{1.5}}{V\Delta t^4_{sub}}$$

where

$\frac{\Delta\rho}{\rho} \times 100$ = per cent density change over that of water at the designated water temperature.

$\frac{q''}{q''_o}$ = ratio of the heat flux in the boiling region to the heat flux at the inception of boiling for the same velocity and subcooling.

V = water velocity, fps.

Δt_{sub} = temperature of subcooling defined as the temperature of saturation minus the temperature of the water, F.

The derivation and discussion of this formula are given in Appendix B.

UCLA collected density data of water during local boiling for pressures of 500 to 2000 psia, mass flow rate of 3,840,000 pounds per hr sq ft (20 fps at 400F), subcooling of 10 to 80F, and heat fluxes of 0 to 1,500,000 Btu per hr sq ft. The data were obtained by measuring the attenuation of X-rays as they passed through an electrically heated stainless steel tube, 0.226 inches nominal inside diameter. The temperature of the water where the density was measured was calculated from the inlet temperature, heat flux, mass rate of flow, and the properties of water under the conditions of operation. It was difficult to control the heat flux, flow, and inlet temperature to give a constant subcooling at the density station.

Table IX lists the density data.

The fluid density data with local boiling at 2000 psi for constant water temperatures of 552, 600, and 620F were plotted as shown in Figure 35. A density change at 620F was indicated, but no definite conclusions were warranted from the data reported.

The density data at pressures of 2000, 1000, and 500 psia were plotted as shown in Figure 36. The ratio of the measured heat flux to the heat flux at the inception of boiling was selected as the abscissa in order to eliminate in some degree the effect of subcooling, which was not held constant. The heat flux at the inception of boiling was calculated from the following formula, using the measured velocity and subcooling.

$$q''_o = h_c(\Delta t_{sat} + \Delta t_{sub})$$

where

q''_o = heat flux at the inception of boiling, Btu per hr sq ft

h_c = heat transfer coefficient as given by the Colburn equation, Btu per hr sq ft F

Δt_{sat} = temperature difference between heated wall temperature and saturation temperature, F

(Formula given in section on local boiling)

Δt_{sub} = temperature difference between the saturation temperature and the bulk water temperature, F

The trend of the data indicates larger density changes at lower pressure. It was observed that the data at lower pressures where density changes occur are reliable to plus or minus 10 per cent density change.

VIII CONCLUSIONS

(1) The forced convection heat transfer coefficient for water flowing in a round or square tube was unaffected by dissolved gases. The coefficient may be predicted with the Colburn equation:

$$N_{Nu}\, N_{Pr}^{-1/3} = 0.023\, N_{Re}^{0.8}$$

within plus or minus 20 per cent for a clean smooth surface with Reynolds numbers greater than 50,000.

(2) Wall temperatures during local boiling with forced flow for nickel and stainless steel surfaces may be predicted within plus or minus 14F with the relation

$$\Delta t_{sat} = \frac{60\left(\frac{q''}{10^6}\right)^{1/4}}{e^{\frac{P}{900}}}$$

(3) The formula given below for burnout correlates the UCLA data to within plus 23 per cent and Purdue data within plus 60 per cent. The values

of the constants "C" and "m" vs. pressure are given in Figure 24 and in the table which follows the formula

$$\frac{q''}{10^6} = C\left(\frac{G}{10^6}\right)^m (t_{sat} - t_b)^{0.22}$$

VALUES OF "m" AND "C" VS. PRESSURE

Pressure, psia	"m"	$\frac{C}{10^6}$ (UCLA)	$\frac{C}{10^6}$ (Purdue)
500	0.16	0.817	--
1000	0.275	0.626	0.915
2000	0.500	0.445	0.545
3000	0.725	--	0.300

The burnout tests with net steam generation were all for constant inlet velocities. This condition of constant velocity would probably not exist in parallel flow channels, with one channel generating net steam. For use in design calculations, burnout data with net steam generation are not complete unless pressure drop data are also known. Similarly, the pressure drop with local boiling is needed to complete the burnout data with subcooling.

(4) Pressure drop with treated water, gas free, can be predicted up to the point of incipient boiling to within plus or minus 10 per cent, using Moody's (5) friction factor data. Lack of data prohibits prediction of the effects of dissolved gases on pressure drop at low subcoolings.

(5) A limited amount of density data from UCLA indicates no appreciable change in density for subcoolings as low as 16F and heat fluxes up to 1,000,000 Btu per hr sq ft at 2000 psia. At 1000 and 500 psia pronounced density changes were measured for subcoolings below 20F during local boiling.

IX APPENDICES

A. Curves and Tables of Data

Forced Convection Heat Transfer - Figures 1 through 13 inclusive.

Local Boiling Heat Transfer - Figures 14 through 18 inclusive and Table I.

Burnout Heat Flux - Tables II and III, Figures 19 through 24 inclusive, and Tables IV and V

Pressure Drop with High Water Temperatures - Table VI, Figures 25, 26, 27, Table VII, Figures 28 through 33 inclusive, Table VIII, and Figure 34.

Density of Water and Water Vapor Mixtures During Local Boiling - Table IX and Figures 35 and 36.

NR-G-2537-B

FIG. 1
EFFECT OF OPERATING CONDITIONS ON THE SCALING OF ELECTRICALLY HEATED TUBES (REPRODUCED FROM DATA OBTAINED AT UCLA)

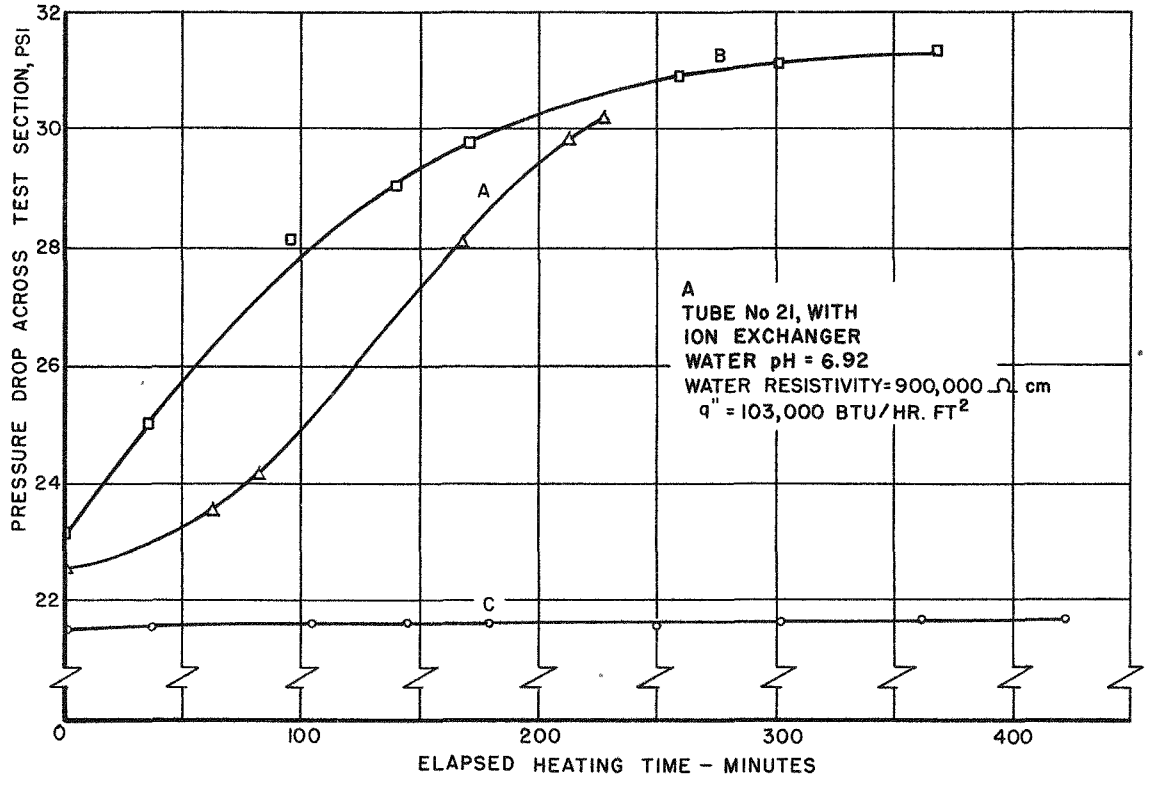

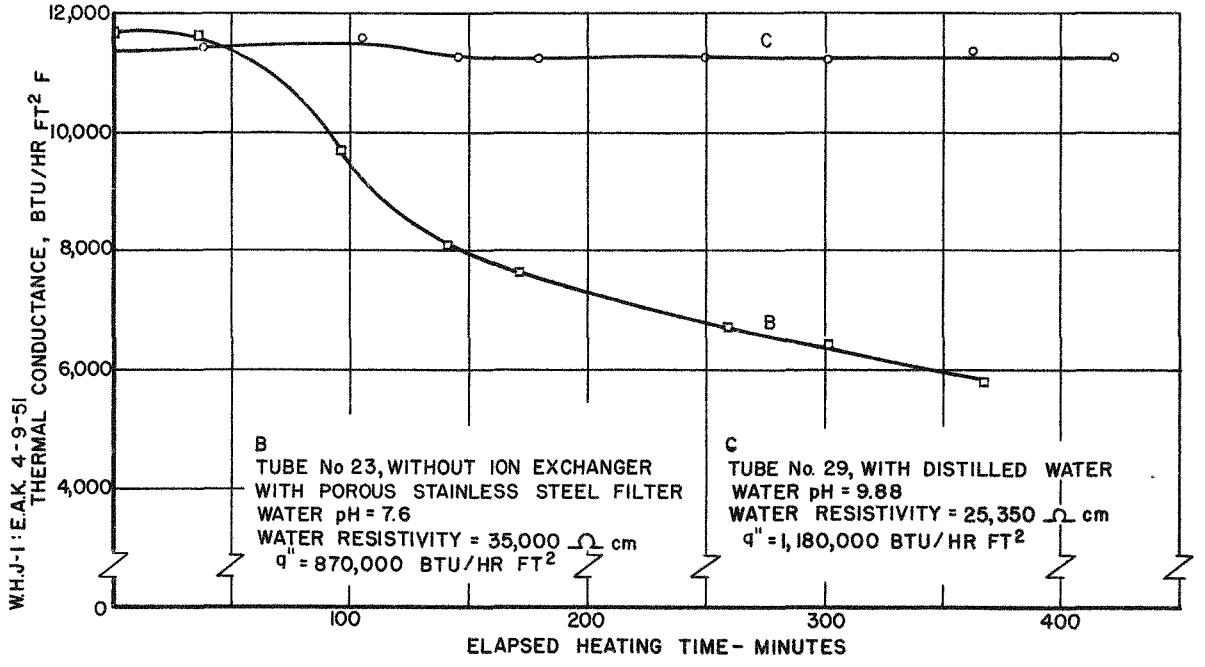

568-24

FIG. 2
TYPICAL LOCAL HEAT TRANSFER COEFFICIENTS AND TEMPERATURE DISTRIBUTIONS ALONG A UCLA HEATED TUBE (RUN 448)

NR-G-2530-A

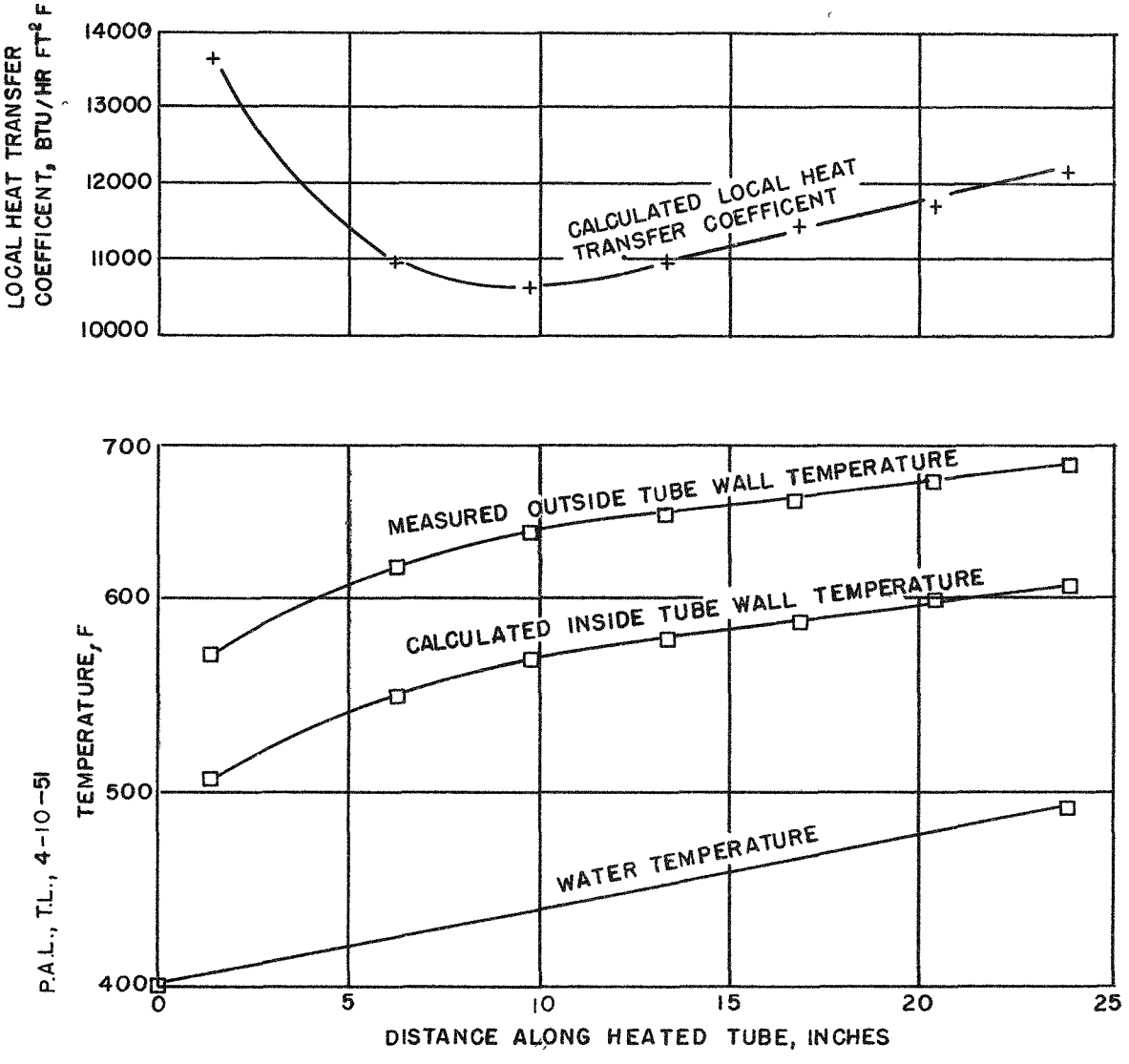

568-25

P.A.L.- P.J.B. 4-13-51

FIG. 3

COMPARISON OF UCLA HEAT TRANSFER DATA WITH THE COLBURN EQUATION (WITHOUT PH CONTROL- DATA CORRELATED BY UCLA)

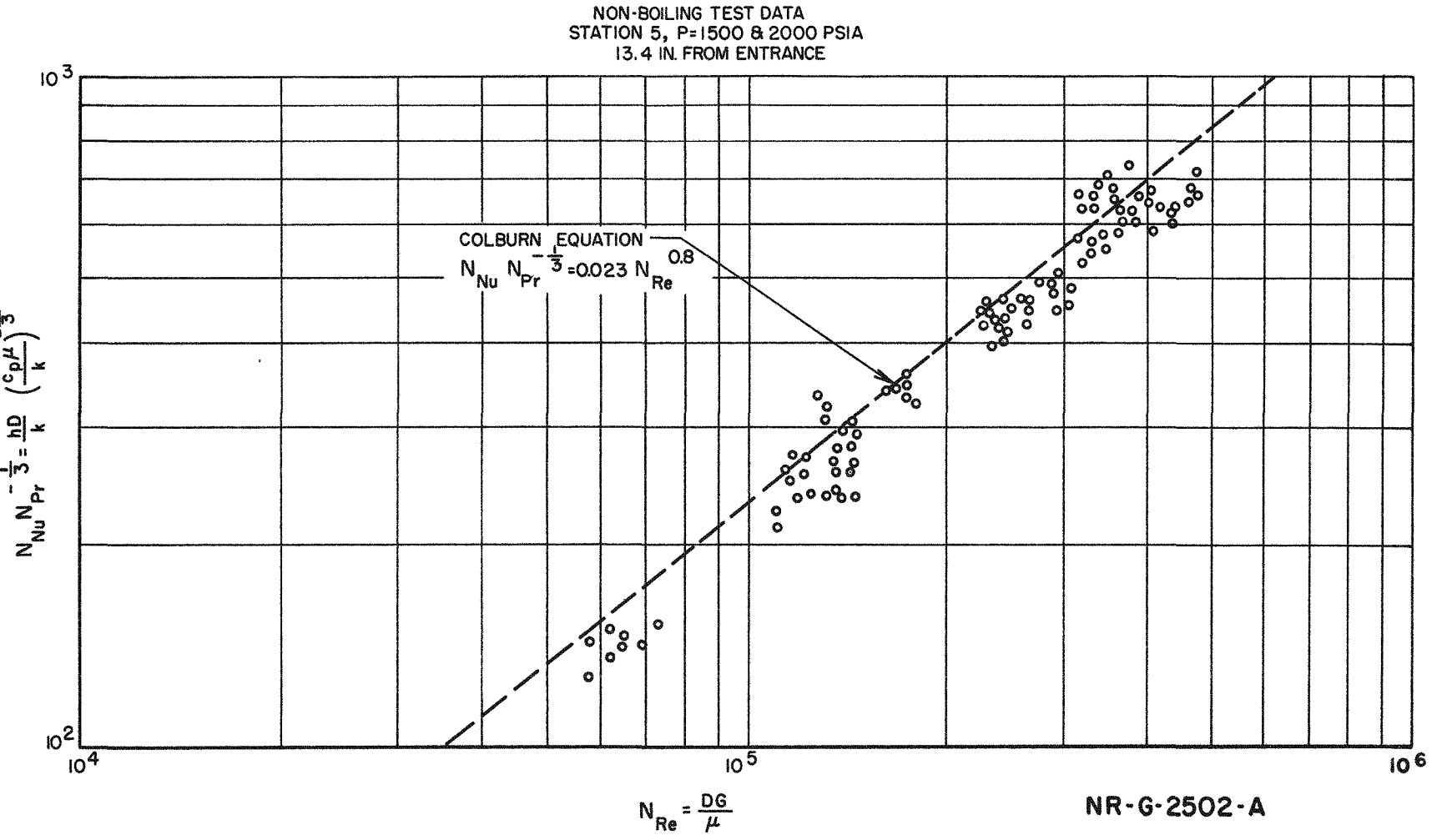

P.A.L.-P.J.B. 4-13-51

29

FIG. 4
COMPARISON OF UCLA TEST DATA WITH THE COLBURN EQUATION (WITH PH CONTROL)

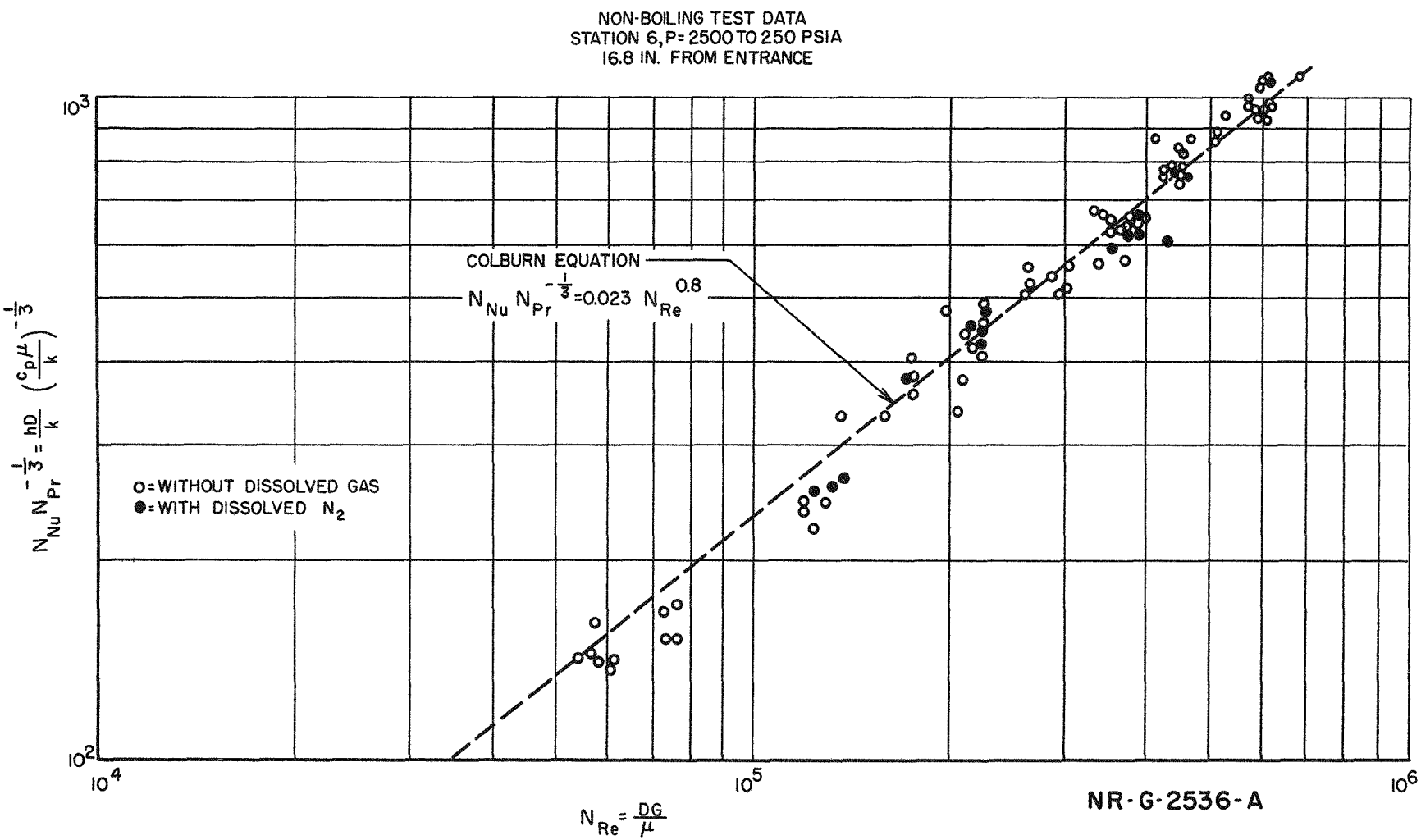

FIG. 5
TYPICAL MIT HEAT TRANSFER DATA AT 2000 PSIA AND MASS FLOW RATE OF 5.73×10^6 LB./HR SQ. FT.

NR-G-2533-A

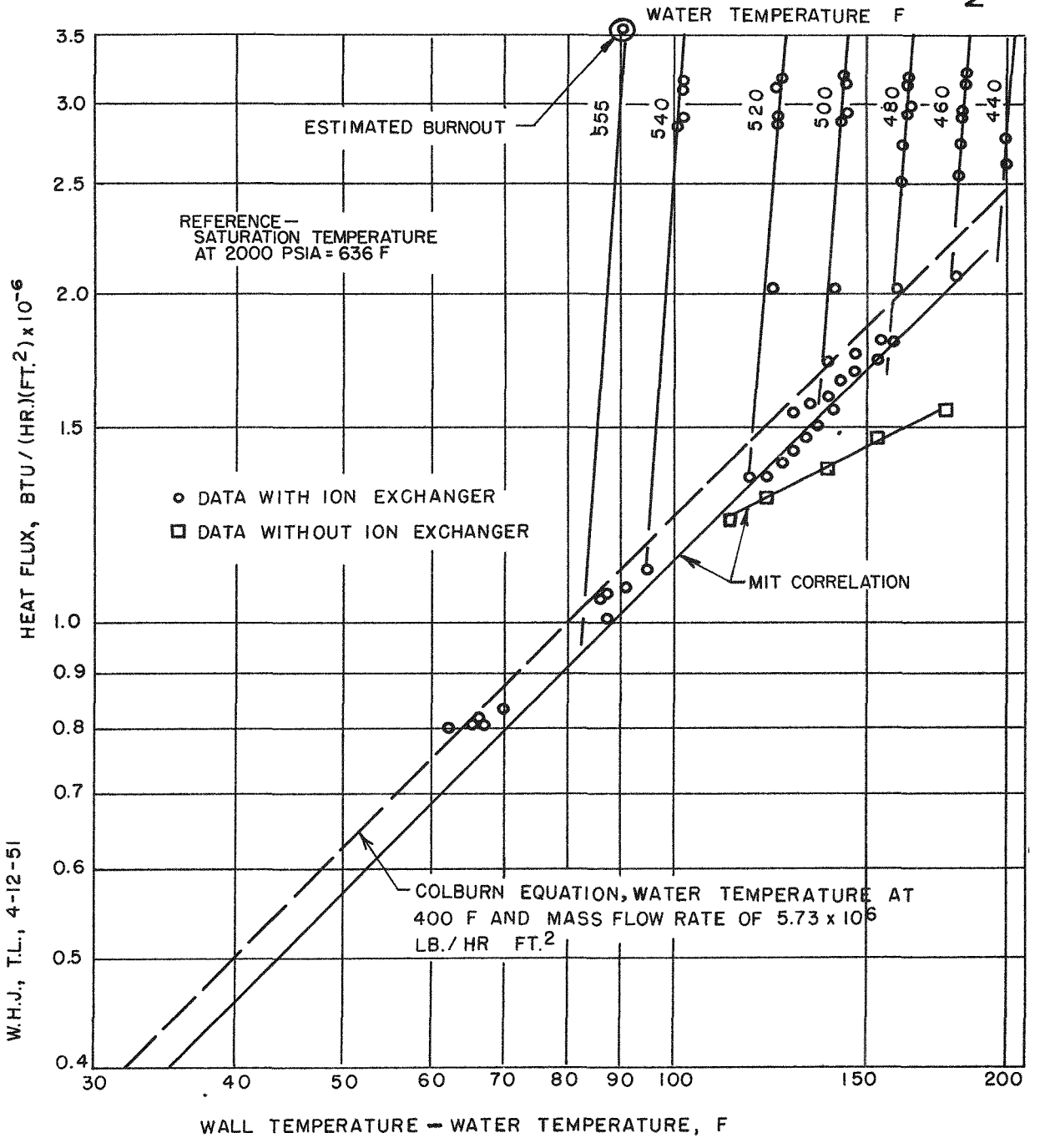

FIG. 6
COMPARISON OF MIT LOW VELOCITY HEAT TRANSFER DATA WITH THE COLBURN EQUATION

NON-BOILING TEST DATA P=2000 PSIA

NR-G-2503-A

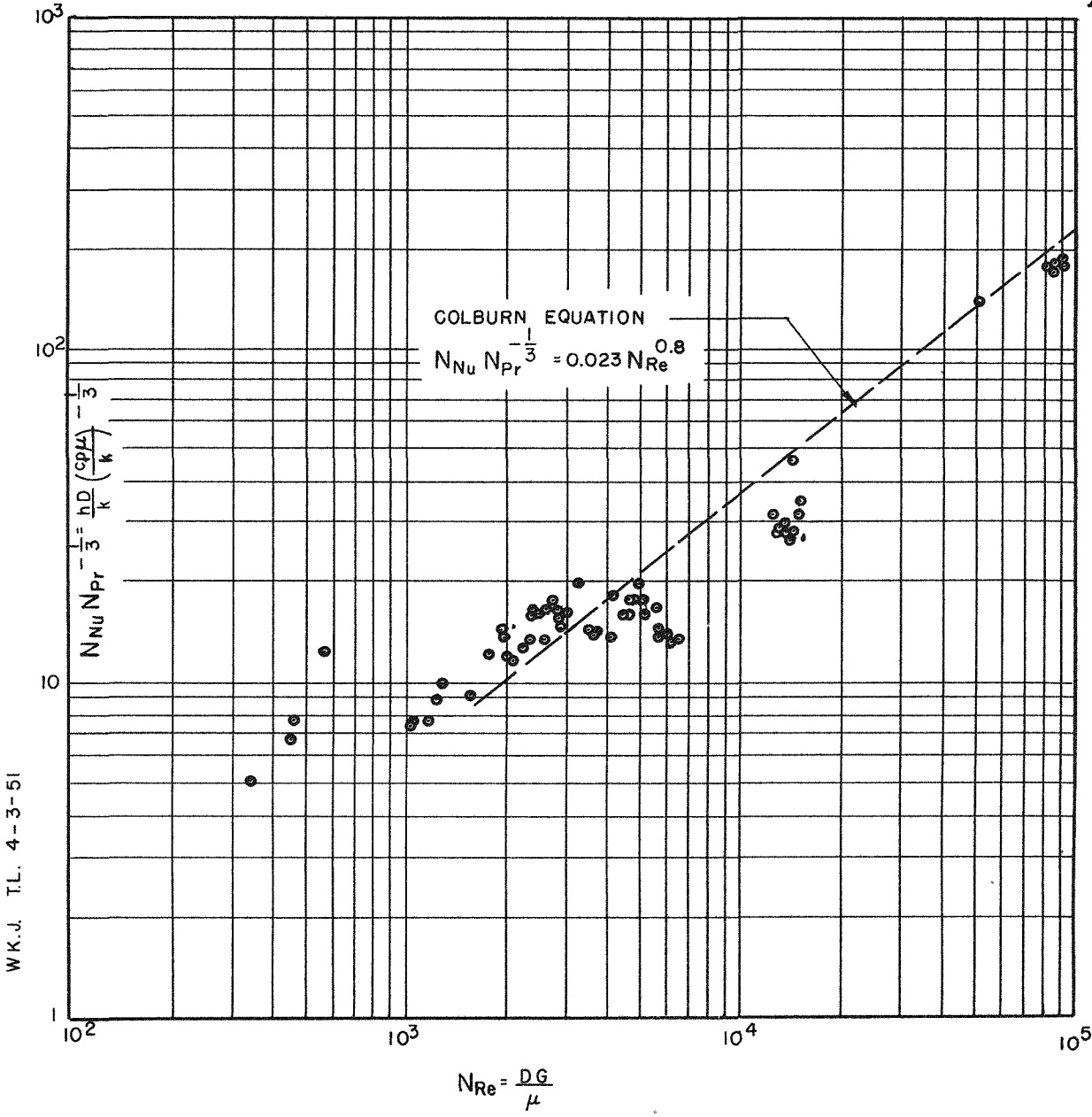

W.K.J. T.L. 4-3-51

5 68-29

W.H.J.-P.J.B. 4-4-51

FIG. 7

COMPARISON OF MIT HEAT TRANSFER DATA WITH THE COLBURN EQUATION FOR POSITION-DIAMETER RATIO OF 10

NON-BOILING TEST DATA
STATION 2, P=2000 & 1500 PSIA

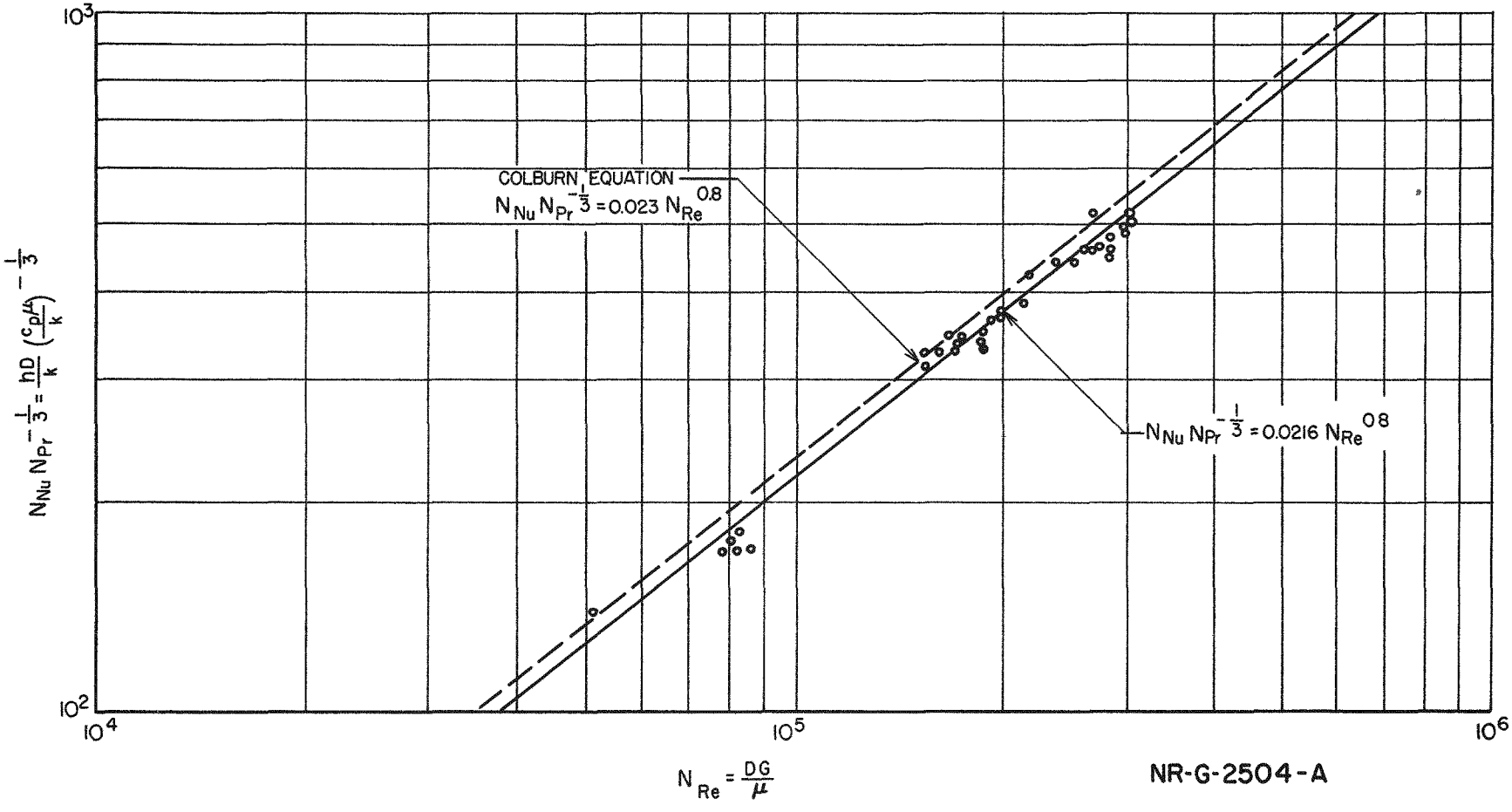

W.H.J. T.L. 4-5-51

FIG. 8
COMPARISON OF MIT HEAT TRANSFER DATA WITH THE COLBURN EQUATION FOR POSITION-DIAMETER RATIO OF 18

NON-BOILING TEST DATA
STATION 3, P = 2000 & 1500 PSIA

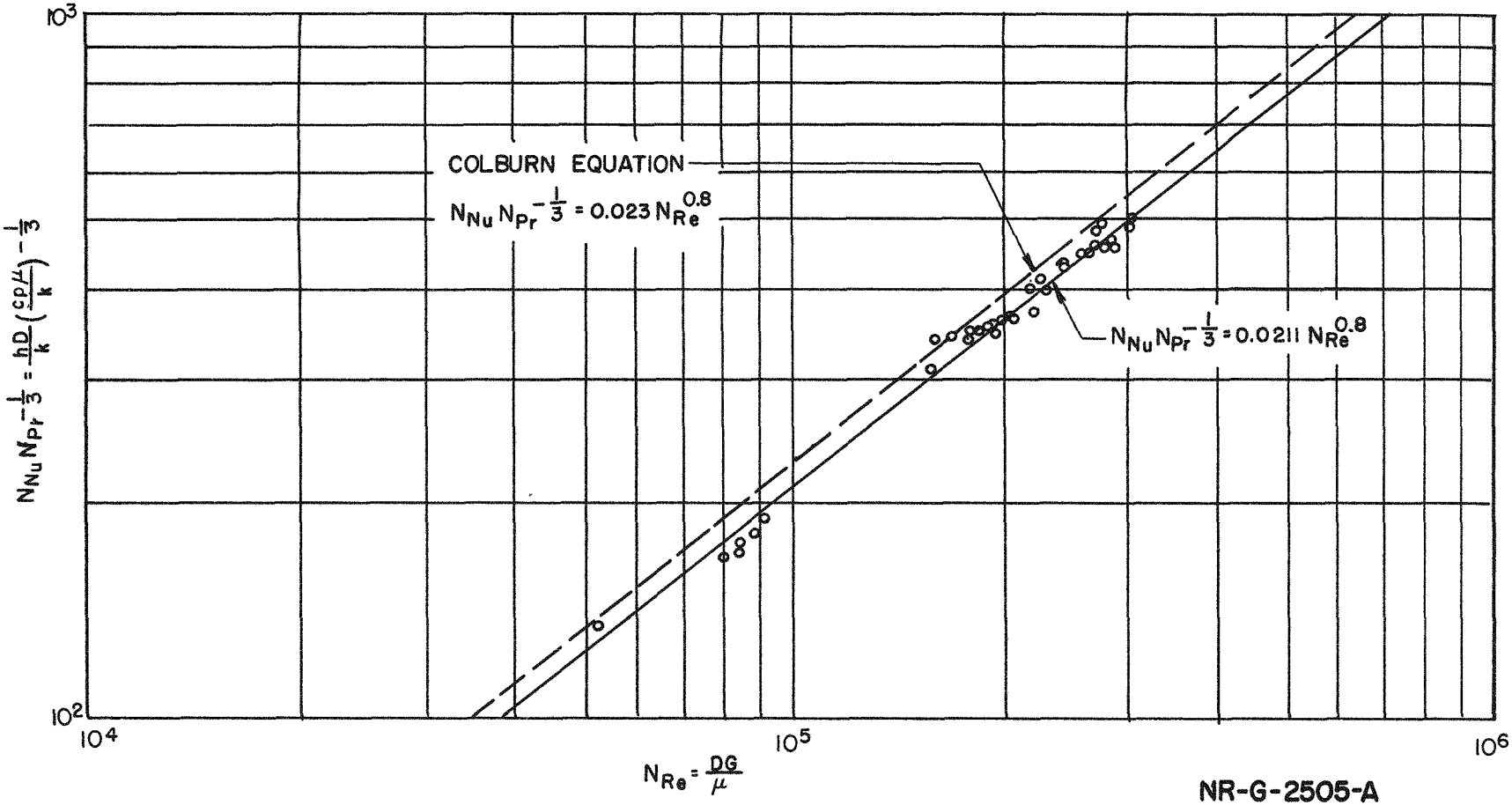

NR-G-2505-A

W.H.J.-P.J.B. 4-4-51

FIG. 9
COMPARISON OF MIT HEAT TRANSFER DATA WITH THE COLBURN EQUATION FOR POSITION-DIAMETER RATIO OF 25

NON-BOILING TEST DATA
STATION 4, P=2000 & 1500 PSIA

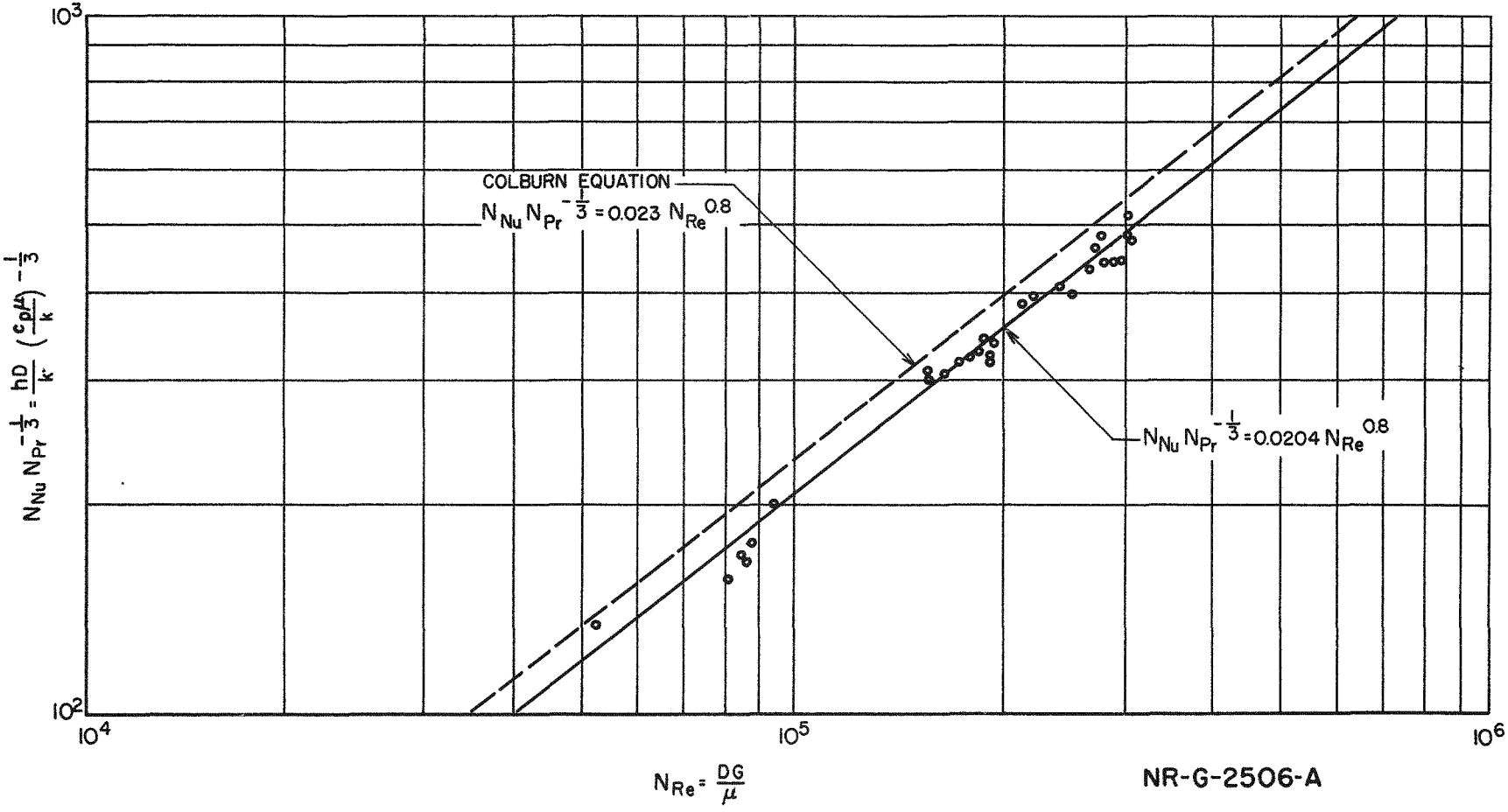

W.H.J. T.L. 4-5-51

FIG. 10
COMPARISON OF MIT HEAT TRANSFER DATA WITH THE COLBURN EQUATION FOR POSITION-DIAMETER RATIO OF 33

NON-BOILING TEST DATA
STATION 5, P = 2000 & 1500 PSIA

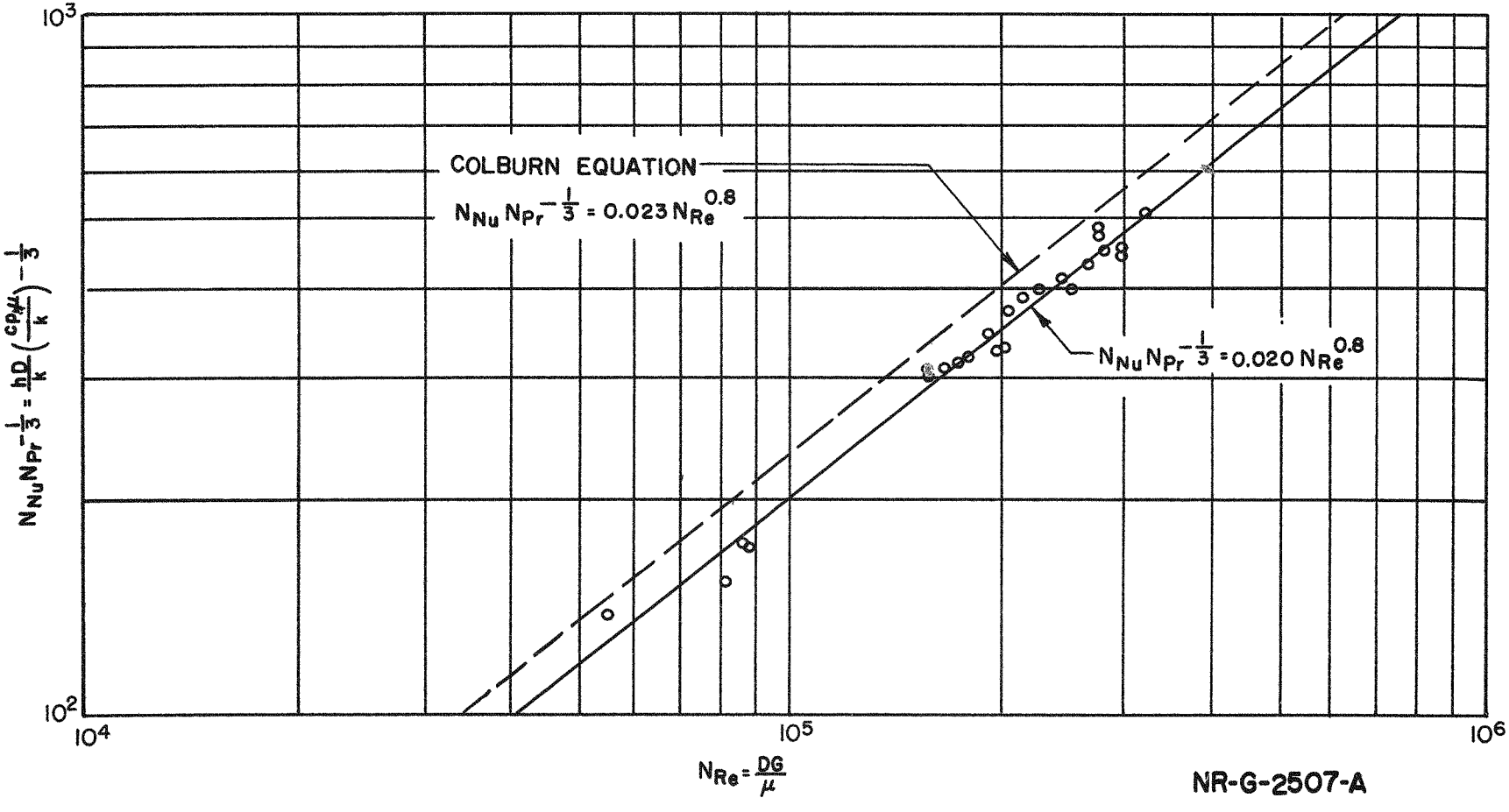

W.H.J.-P.J.B 4-4-51

FIG. 11
COMPARISON OF MIT HEAT TRANSFER DATA WITH THE COLBURN EQUATION FOR POSITION-DIAMETER RATIO OF 41

NON-BOILING TEST DATA
STATION 6, P=2000 & 1500 PSIA

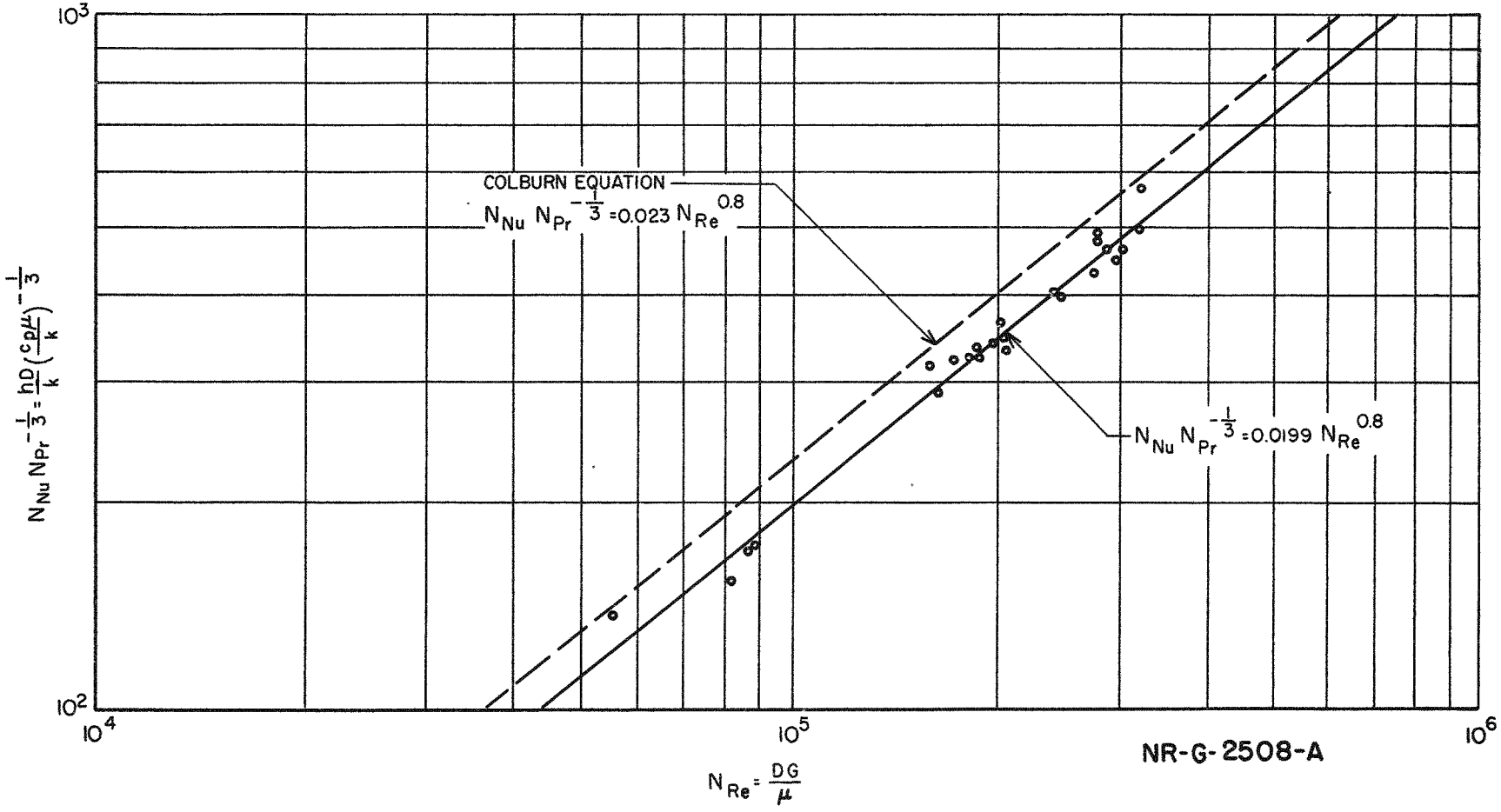

W.H.J. T.L. 4-4-51

FIG. 12
MIT HEAT TRANSFER DATA: LOCAL VALUES OF "C" IN THE CONVECTION EQUATION, $N_{Nu} N_{Pr}^{-\frac{1}{3}} = C N_{Re}^{0.8}$, ALONG THE HEATED TUBE.

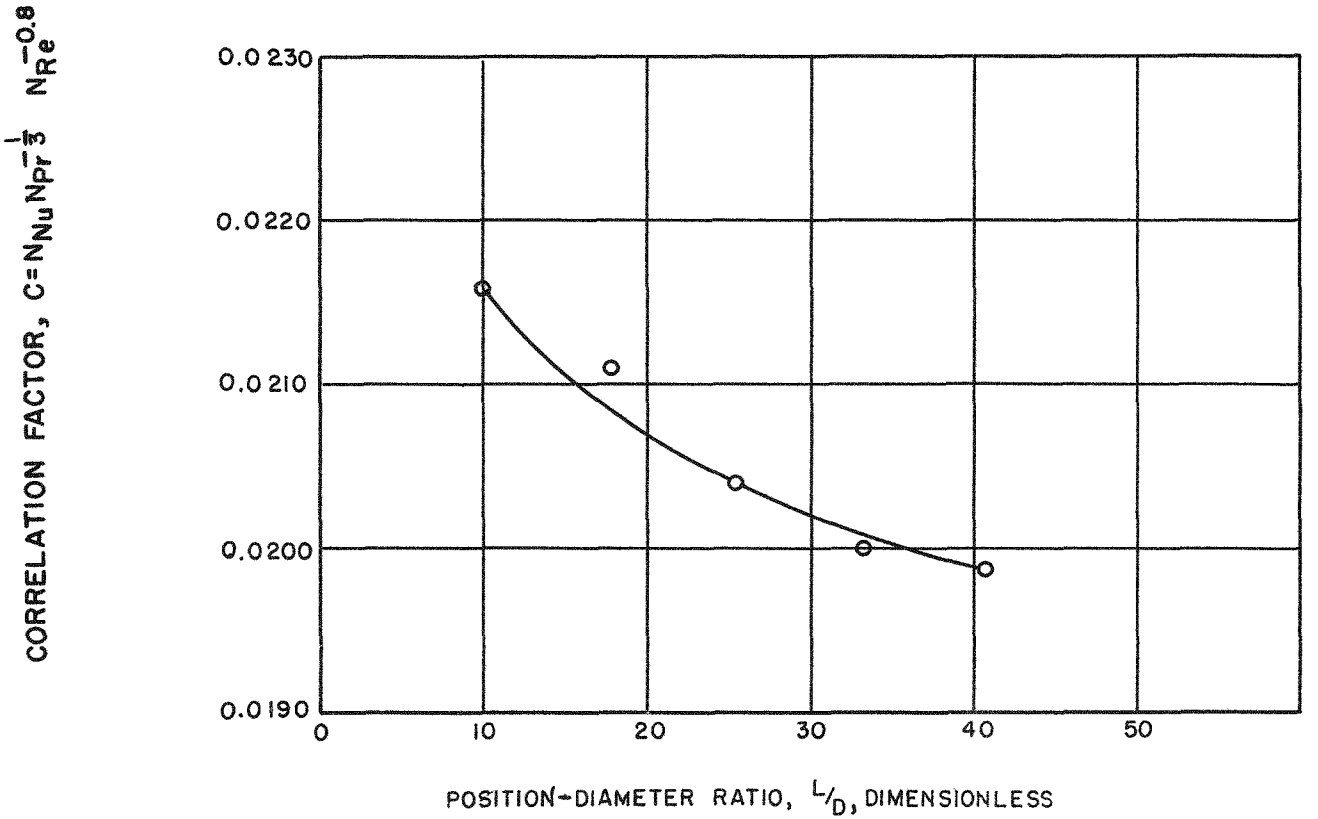

NR-G-2509-A

P.A.L.-P.J.B. 4-4-51

FIG. 13

COMPARISON OF PURDUE HEAT TRANSFER DATA WITH THE COLBURN EQUATION FOR TREATED BOILER WATER
(DATA CORRELATED BY PURDUE)

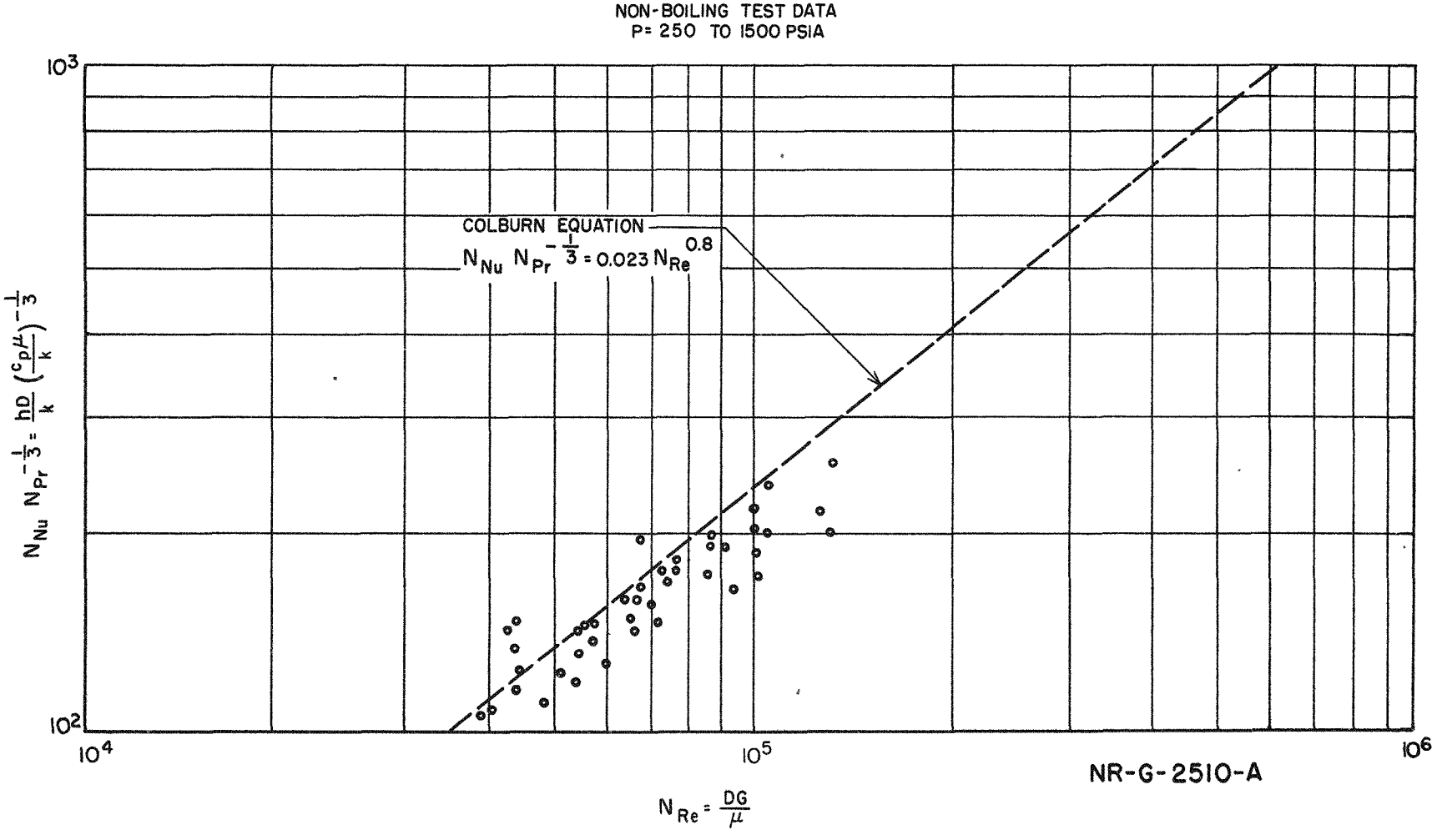

FIG. 14
UCLA LOCAL BOILING HEAT TRANSFER DATA WITH DISSOLVED GAS

PRESSURE = 2000 PSIA
MASS FLOW RATE = 1.93×10^6 LBS/HR. FT^2
750cc N_2 / LITER H_2O
RUNS 570-581
PH = 9.69

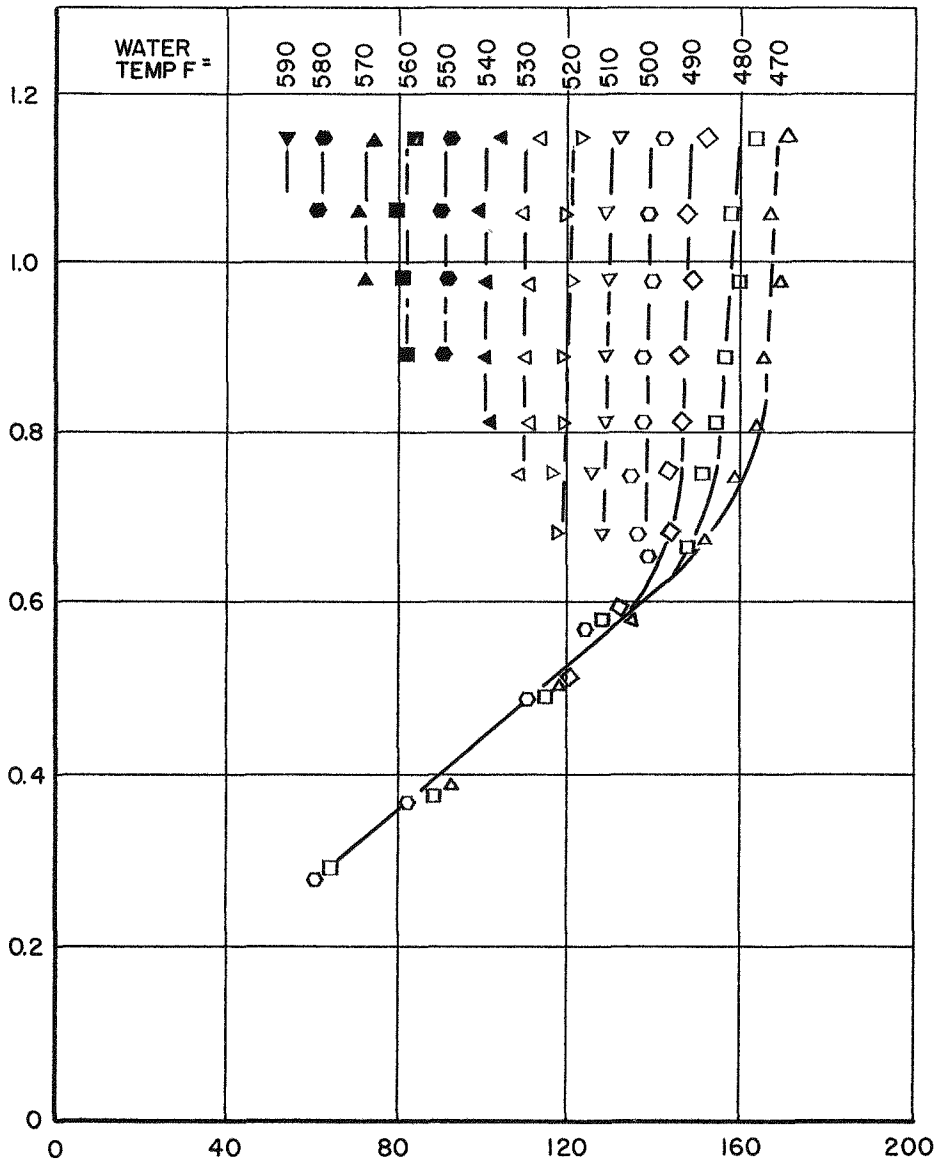

W.H.J.-P.J.B. 4-17-51

NR-G-2534-A

FIG. 15
UCLA LOCAL BOILING HEAT TRANSFER DATA WITHOUT DISSOLVED GAS

PRESSURE = 2000 PSIA
MASS FLOW RATE = 1.93×10^6 LB./HR. FT.^{2}
RUNS 558-569
PH = 9.69

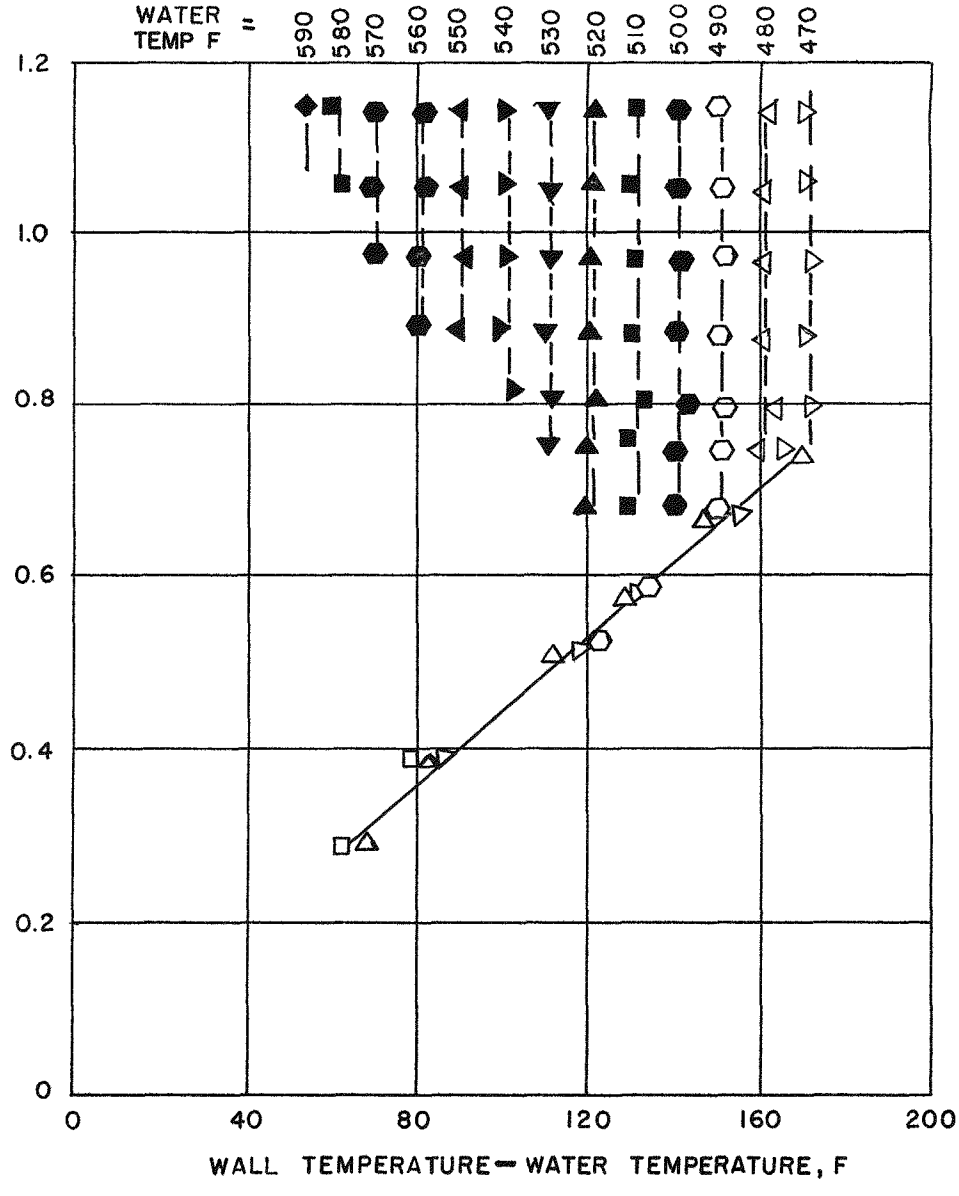

W.H.J., T.L., 4-17-51

FIG. 16
UCLA LOCAL BOILING DATA: EFFECT OF HEAT FLUX ON WALL SUPERHEAT AT 500 PSIA

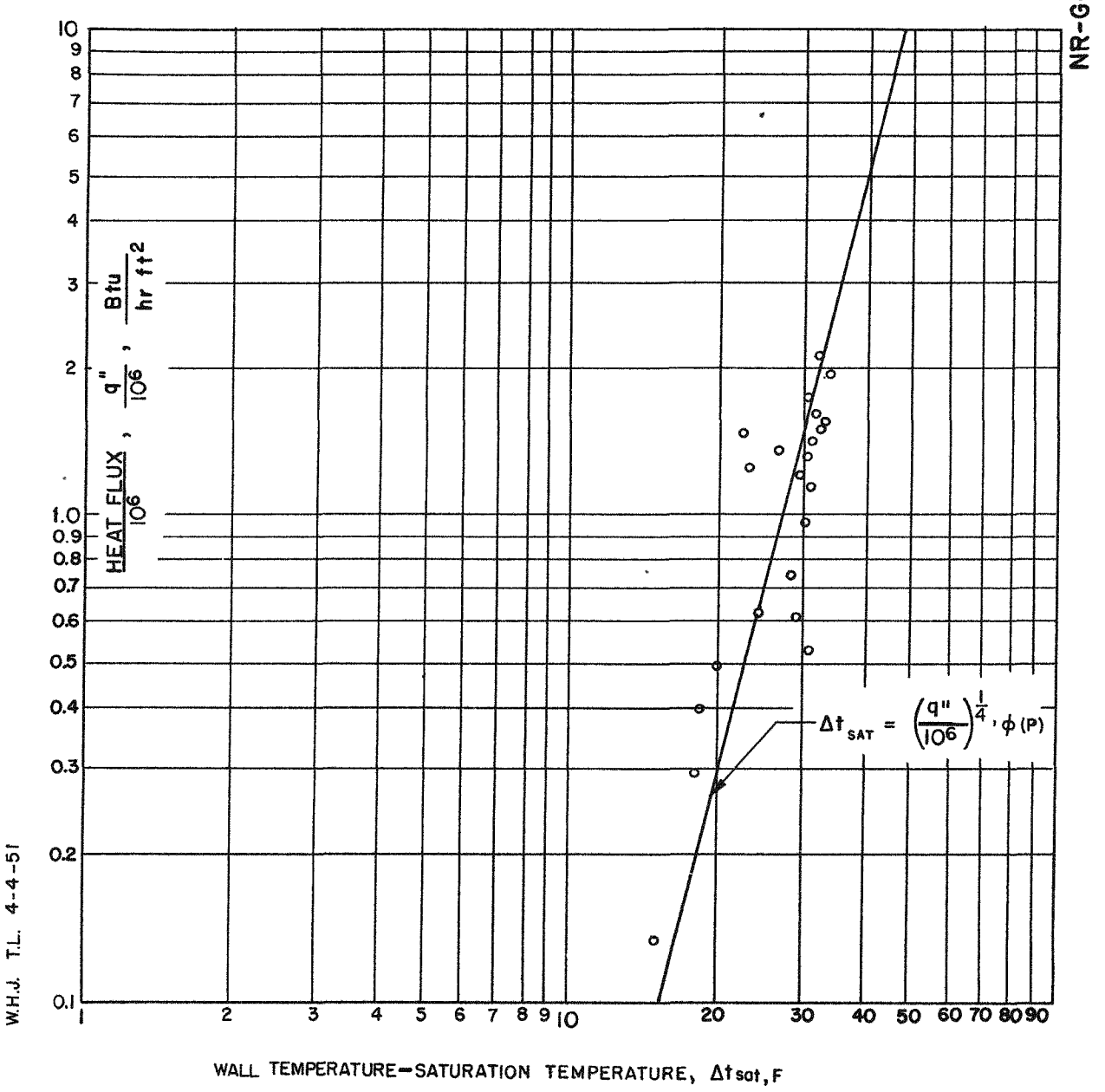

568 - 39

NR-G-2512-A

FIG. 17

UCLA LOCAL BOILING DATA: EFFECT OF PRESSURE ON WALL SUPERHEAT

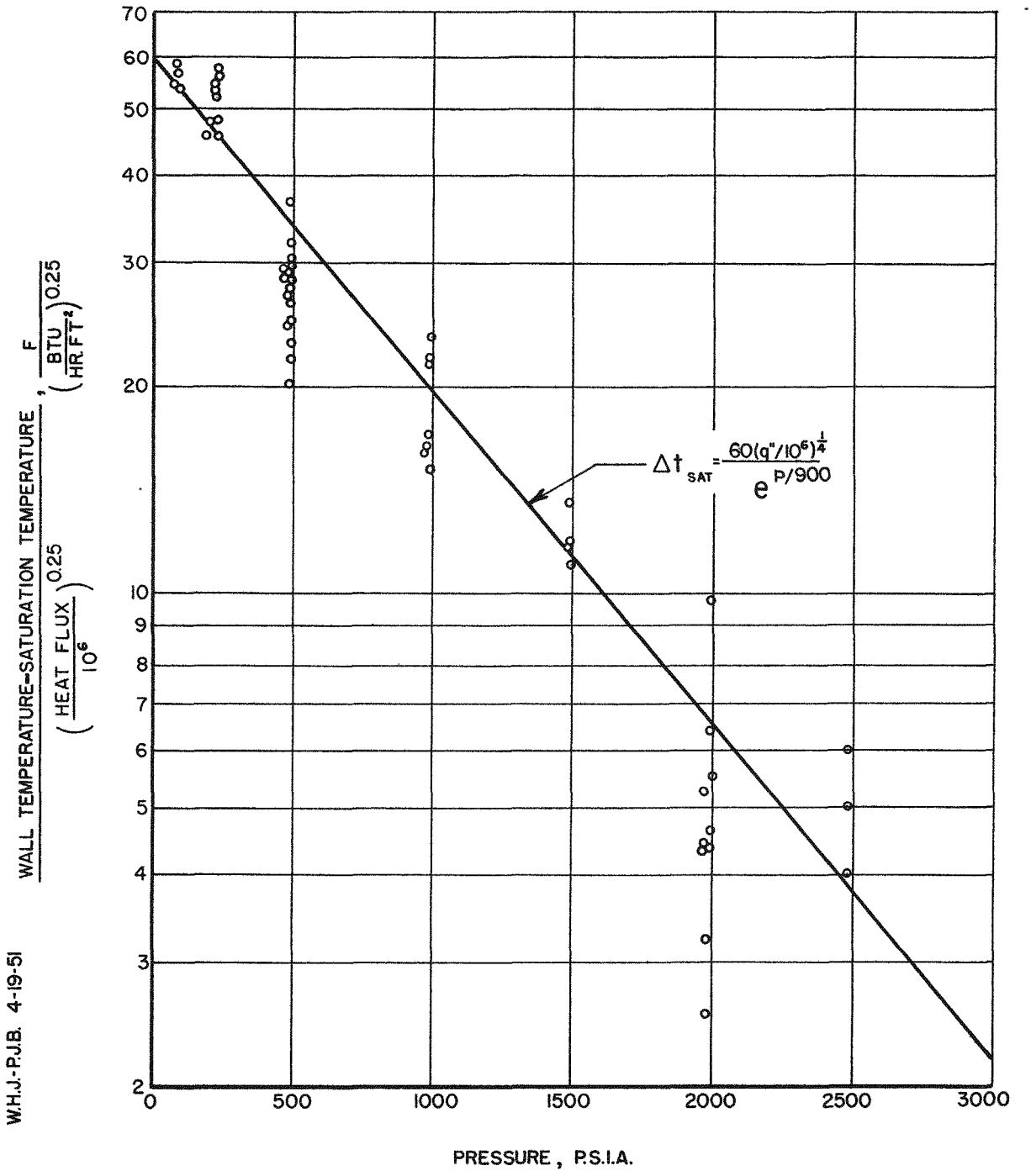

W.H.J.-P.J.B. 4-19-51

568-111

NR-G-2513-A

FIG. 18
MIT LOCAL BOILING DATA: EFFECT OF PRESSURE ON WALL SUPERHEAT

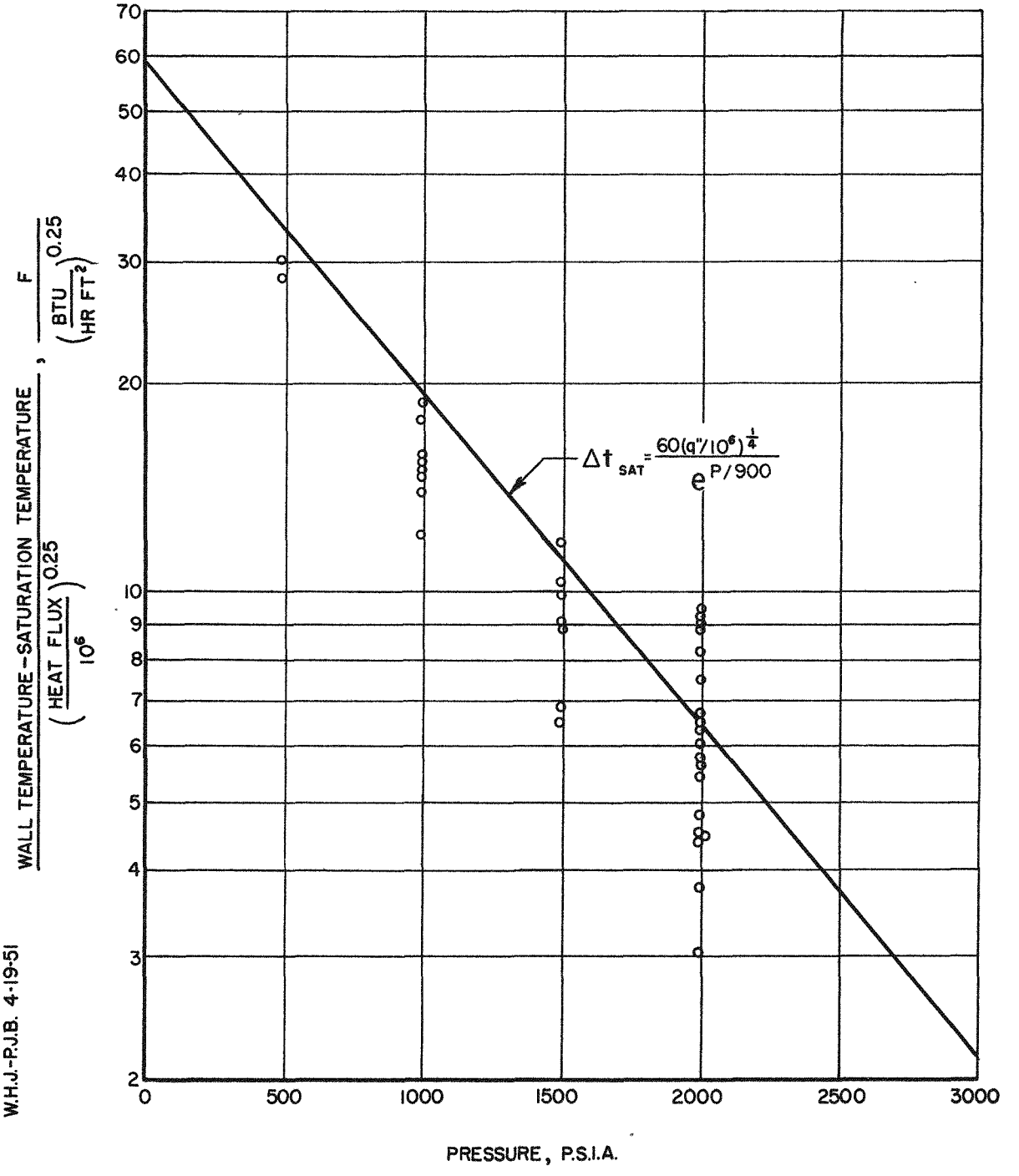

TABLE I - EFFECT OF GAS CONTENT ON WALL SUPERHEAT, Δt_{sat}, UCLA LOCAL BOILING DATA

Run No.	Gas Addition to Water, cc N_2/Liter	Water Mass Flow Rate x 10^{-6} lb/hr sq ft	Entrance Water Temp., F	Pressure, psia	Δt_{sat}	Point of Inception of Boiling
445-456	0	5.73	400	2000	2	-
457-463	280	5.73	400	2000	0	Identical with zero gas runs
504-508	565	5.73	400	2000	0	No curves available for comparison
558-569	0	1.91	400	2000	6	-
570-581.1	750	1.91	400	2000	2	Identical with zero gas runs
464-474	0	5.73	500	2000	4	-
486-496	335	5.73	500	2000	6	Identical with zero gas runs
476-485	465	5.73	500	2000	4	No curves available for comparison
511-532	705	5.73	500	2000	5	Identical with zero gas runs
704-714	0	7.65	600	2000	7	-
728-737	720	7.65	600	2000	9	Heat flux 20 per cent lower than run without gas
583-597	0	5.73	600	2000	6	-
598-610	710	5.73	600	2000	2	No curves available for comparison
696-703	0	3.81	600	2000	7	-
720-727.4	770	3.81	600	2000	8	"q" slightly lower with gradual transition to boiling
911-920	0	1.91	600	2000	4	-
738-748	780	1.91	600	2000	9	Identical with zero gas runs
943-951	900	1.91	600	2000	5	No curves available for comparison
820-831	0	3.81	371	500	26	-
902-910	110	3.81	371	500	25	Identical with zero gas runs

TABLE II - UCLA BURNOUT DATA FOR SUBCOOLED WATER AT TUBE EXIT

Run No.	Exit Pressure, psia	Exit Subcooling, F	Mass Flow x 10^{-6}, lb/hr ft^2	Burnout Flux x 10^{-6}, Btu/hr ft^2
651	2000	10	0.97	1.12
652	2000	39	0.96	1.11
654	2000	43	0.97	1.11
655	2000	34	0.97	1.08
656	2000	40	0.97	1.07
657	2000	34	0.97	1.04
658	2000	46	0.97	1.01
659	2000	24	0.97	0.940
667	2000	48	3.92	2.08
668	2000	48	3.90	2.16
669	2000	30	3.88	1.88
670	2000	16	3.87	1.60
671	2000	6.5	3.88	1.42
674	2000	130	3.95	2.92
675	2000	84	3.95	2.38
678	2000	163	3.95	2.96
680	2000	136	3.88	2.83
682	2000	118	3.90	2.52
683	2000	142	3.88	2.65
684	2000	9	7.76	2.39
685	2000	10.5	7.76	2.28
686	2000	5.5	7.79	2.05
687	2000	34	7.72	2.82
688	2000	44	7.27	3.02
689	2000	66	7.74	3.34
690	2000	122	7.74	3.56
691	2000	128	7.74	3.78
889	500	38	3.87	2.50
890	500	35	3.87	2.72
976	1000	41	7.71	2.74
977	1000	23	7.75	2.20
979	1000	50	3.84	2.13
980	1000	12	3.84	1.77
983	500	46	7.65	2.70
984	500	15	7.75	2.13
985	500	11	7.82	1.93
987	500	22	7.56	2.40
988	500	20	7.56	2.24
989	500	10	7.73	2.04
990	500	30	3.87	2.35
991	500	41	3.87	2.51
992	500	53	3.87	2.68
993	500	21	3.87	2.24
995	1000	28	3.87	2.04
996	1000	58	3.87	2.54
1032	1000	11	7.65	2.05
1033	1000	25	7.79	2.54
1035	500	14	3.87	2.28

TABLE III - PURDUE BURNOUT DATA FOR SUBCOOLED WATER AT TUBE EXIT

Run No.	Exit Pressure, psia	Exit Subcooling, F	Mass Flow x 10^{-6} lb/hr ft^2	Burnout Flux x 10^{-6} Btu/hr ft^2
1023A1	2000	70	3.80	3.15
1024	2000	80	2.00	2.09
1024A	2000	80	5.63	4.02
1024A1	2000	87	7.48	4.03
1026	2000	10.5	1.79	1.20
1028	2000	6	5.69	2.45
1029	2000	149	3.82	4.12
1030	1000	86	2.13	3.37
1031	1000	103	2.98	3.57
1040	3000	134	0.99	1.08
1041	2000	39	1.55	2.22
1042	3000	140	5.05	3.67
1046	2000	107	1.70	2.84
1047	3000	83	0.895	2.58
1050	1000	15	0.97	2.53
1053	1000	59	4.54	4.21

TABLE IV - UCLA BURNOUT DATA FOR NET STEAM GENERATION

Run No.	Exit Pressure, psia	Mass Flow x 10^{-6} lb/hr ft^2	Per Cent Steam by Weight	Per Cent Steam by Volume	Burnout Flux x 10^{-6} Btu/hr ft^2
660	2000	0.968	6.0	32	0.775
663	2000	0.968	0.7	5	0.497
672	2000	3.84	2.4	15	1.15
891	500	3.88	2.4	54	1.89
971	500	0.925	2.2	52	1.52
972	1000	0.925	1.9	28.6	0.88
973	1000	0.925	33.5	90.5	0.68
975	1300	0.89	37.0	90	0.55
981	1000	3.88	1.2	20.3	1.23
982	1100	3.89	7.1	58.3	1.08
986	560	7.7	1.2	33.3	1.67
1030	1000	7.7	0.5	8.8	1.61
1031	1000	7.7	1.8	28.3	1.38

NR-G-2514-A

FIG. 19
UCLA BURNOUT HEAT FLUX AT 500 PSIA-
CORRELATION OF UCLA DATA

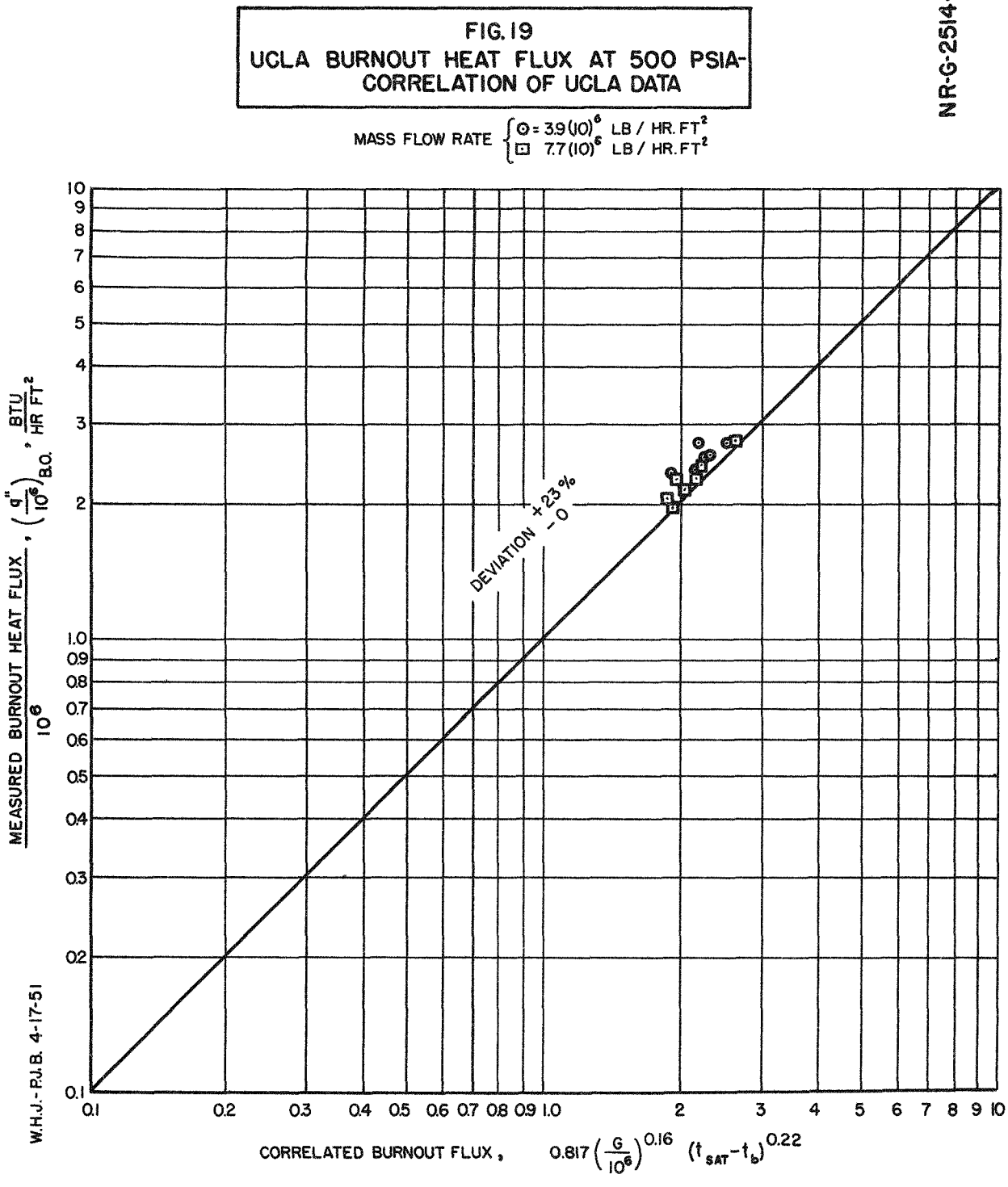

FIG. 20
UCLA BURNOUT HEAT FLUX AT 1000 PSIA
CORRELATION OF UCLA DATA

NR-G 2515-A

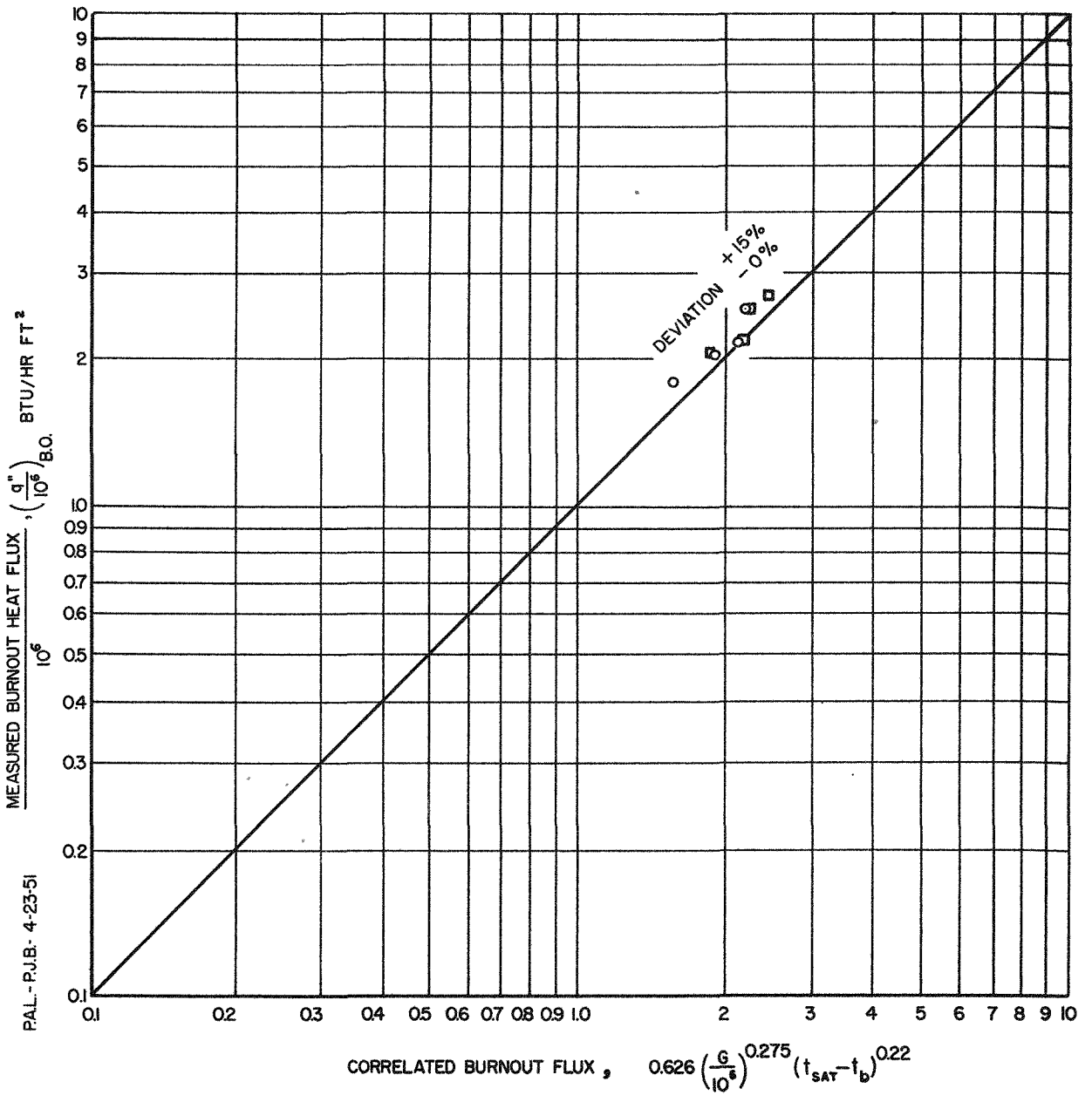

FIG. 21
UCLA BURNOUT HEAT FLUX AT 2000 PSIA
CORRELATION OF UCLA DATA

NR-G 2516-A

MASS FLOW RATES { ○ = 0.97(10)^6 LB/HR FT^2
□ = 3.9(10)^6 LB/HR FT^2
Δ = 7.7(10)^6 LB/HR FT^2

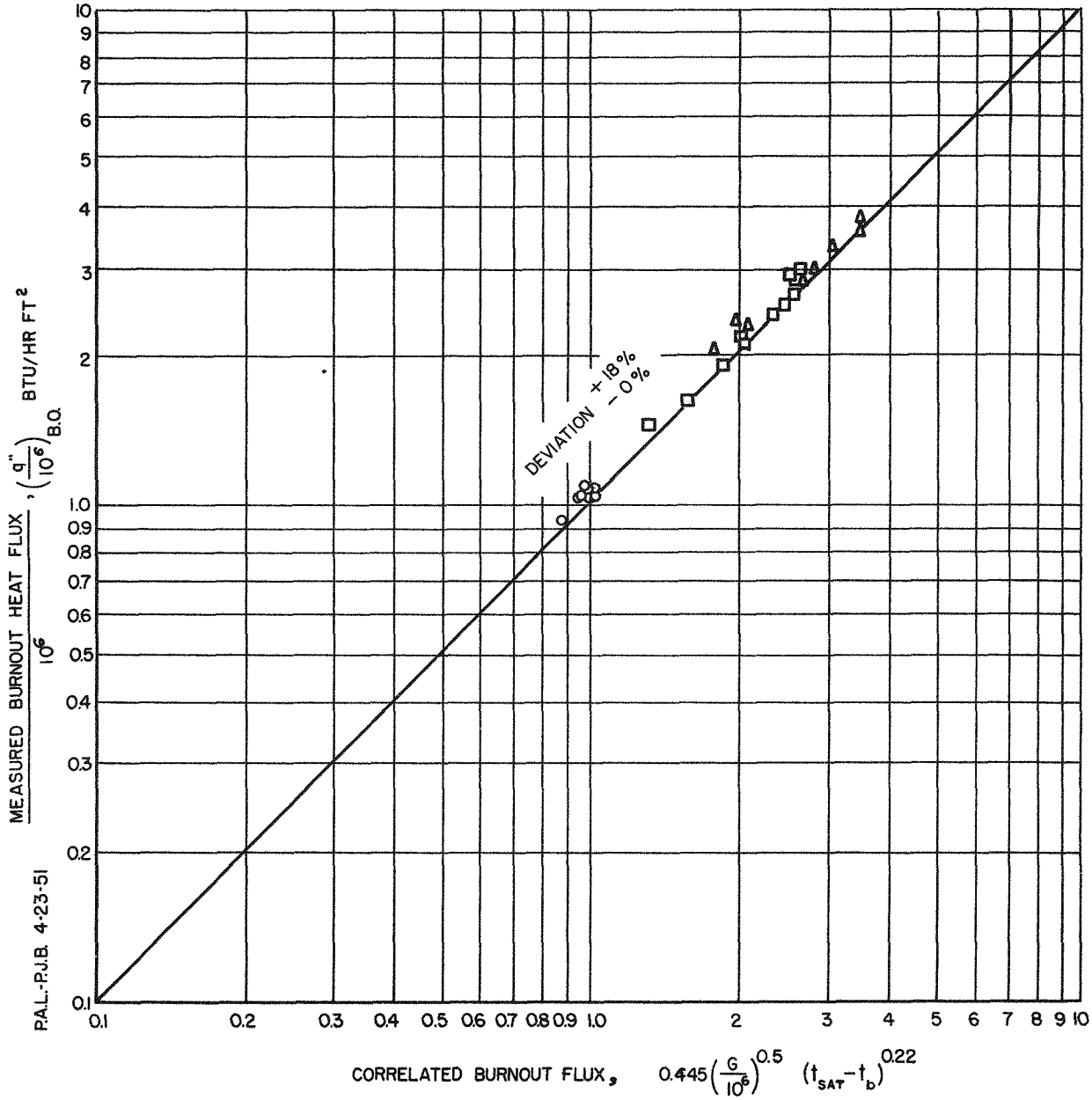

NR-G-2517-A

FIG. 22
UCLA BURNOUT HEAT FLUX AT 500, 1000, AND 2000 PSIA

RANGE OF VARIABLES { PRESSURE 500 TO 2000 PSIA
SUBCOOLING 5 TO 160 F
MASS FLOW $0.9(10)^6$ TO $7.9(10)^6$ LB/HR. FT^2

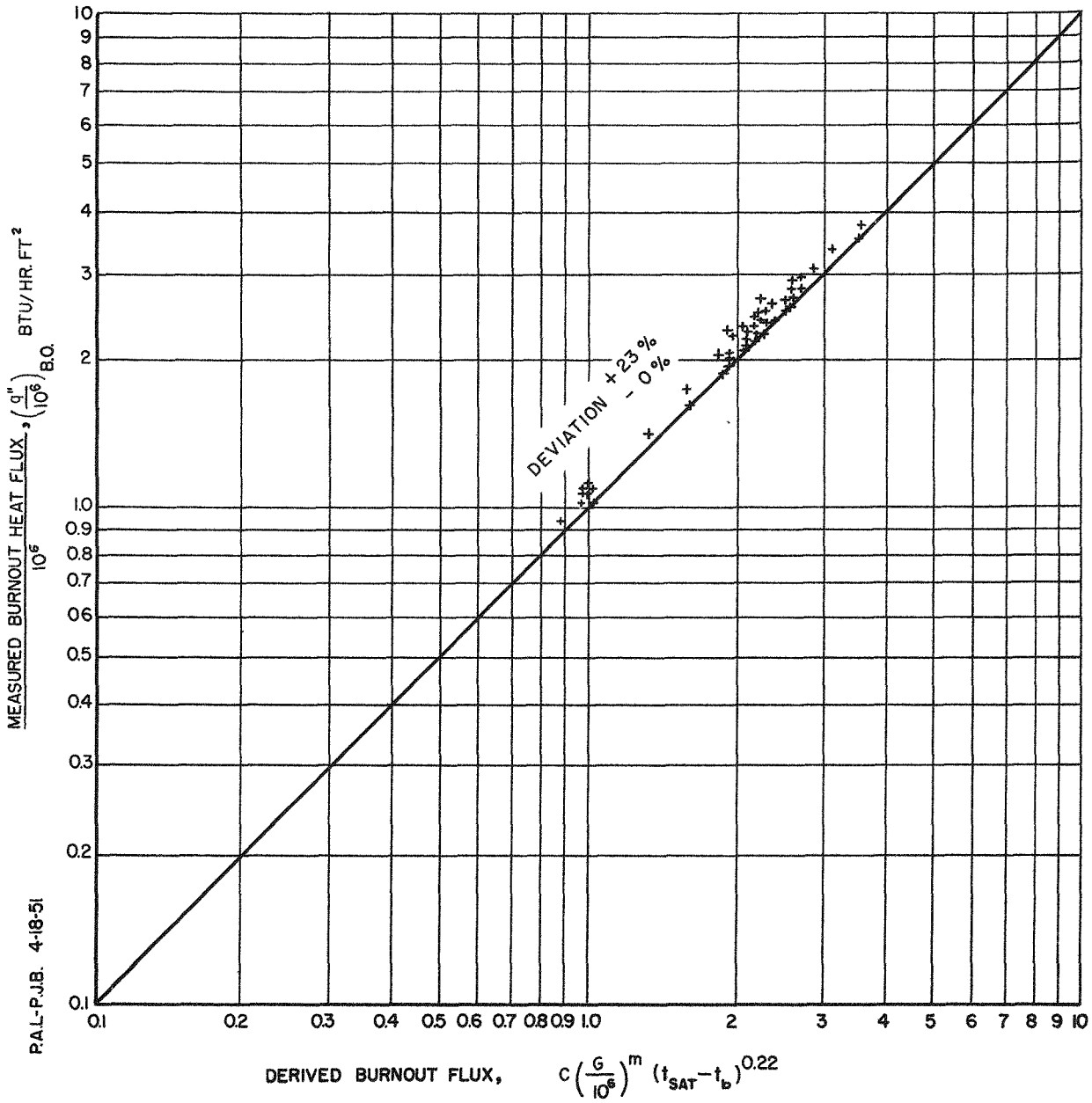

P.A.L.-P.J.B. 4-18-51

568 - 57

NR-G-2518-A

FIG. 23
PURDUE BURNOUT HEAT FLUX AT 1000, 2000, AND 3000 PSIA

RANGE OF VARIABLES { PRESSURE 1000 TO 3000 PSIA
SUBCOOLING 5 TO 150 F
MASS FLOW 10^6 TO $7.5(10)^6$ LB/HR FT^2

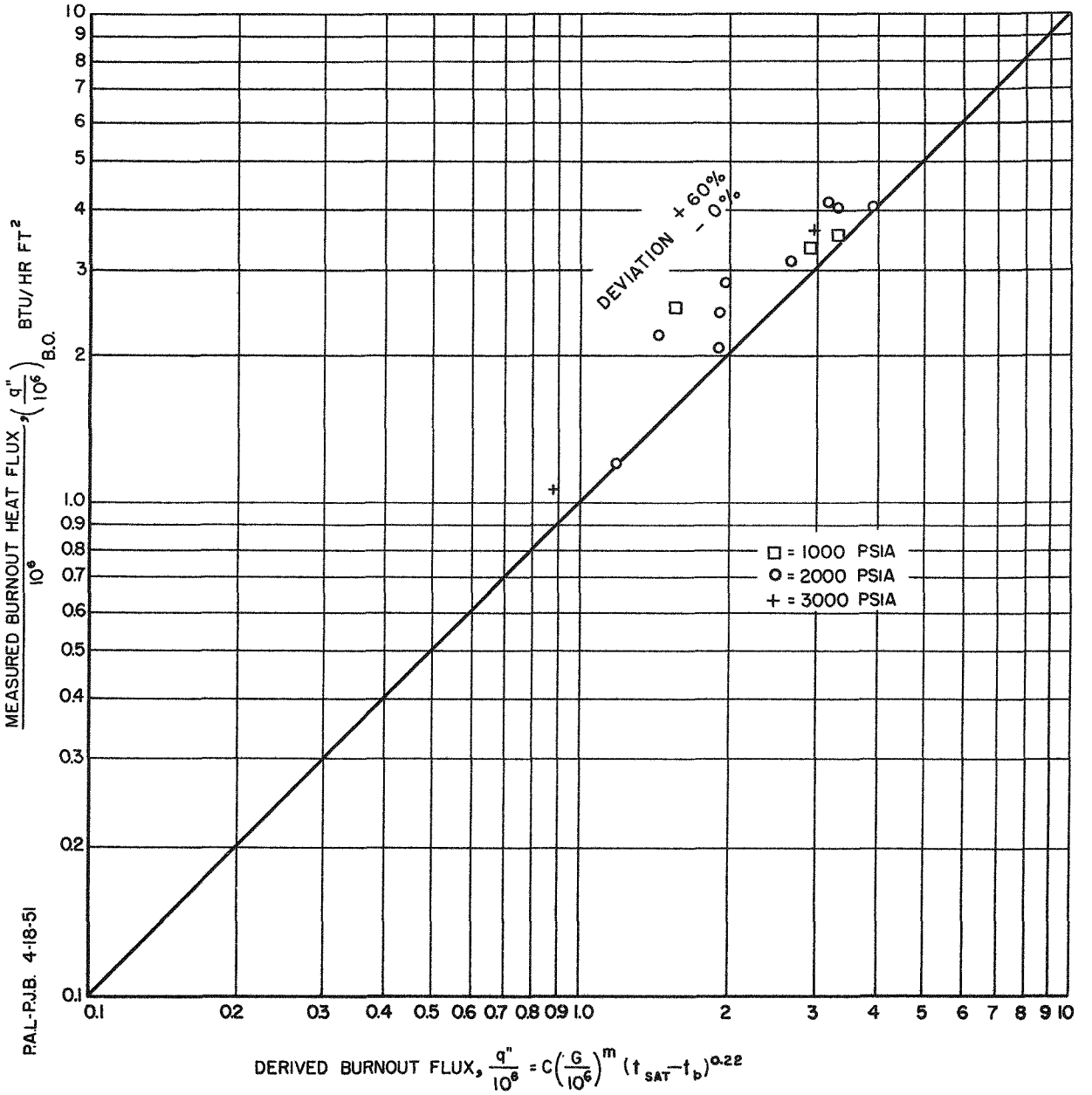

568 - 49

P.A.L., T.L., 4-12-51

FIG. 24
VARIATION OF "C" AND "m" IN THE BURNOUT EQUATION WITH PRESSURE FOR UCLA AND PURDUE BURNOUT HEAT FLUX

NOTE: $m = \phi(P)$ CURVE FROM UCLA DATA WAS ASSUMED TO APPLY TO PURDUE DATA

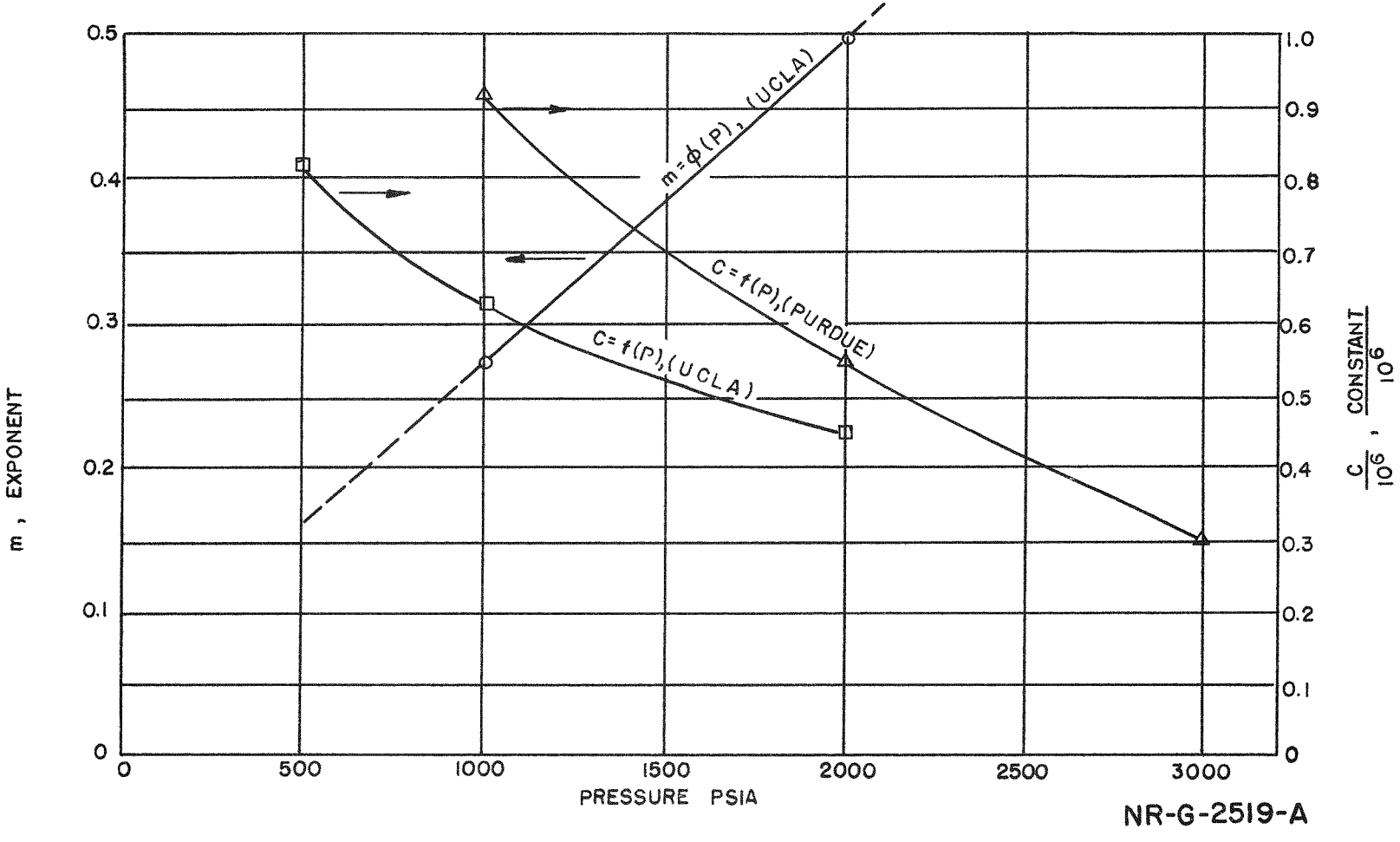

NR-G-2519-A

TABLE V - PURDUE BURNOUT DATA FOR NET STEAM GENERATION

Run No.	Exit Pressure, psia	Mass Flow x 10^{-6} lb/hr ft^2	Per Cent Steam by Weight	Per Cent Steam by Volume	Burnout Flux x 10^{-6} Btu/hr ft^2
1034	2000	5.23	6.8	32.6	1.91
1035	2000	4.27	1.6	9.7	1.59
1036	2000	2.90	4.4	25.6	1.25
1037	2000	1.18	8.3	37.3	1.23
1038	1200	1.10	4.5	42.7	1.02
1045	500	1.10	25	94.0	2.65
1048	280	0.91	31	97.5	3.13
1049	500	0.97	18	91.0	2.85
1051	300	3.36	5.7	82.0	3.56

TABLE VI - UCLA DATA FOR ISOTHERMAL FRICTION FACTORS

Run No.	Tube No.	Water Temperature, F	Reynolds No.	Nitrogen Content, cc/liter	Friction Factor
228	13	607	53,100	-	0.0155
243	13	599	35,200	-	0.0268
244	13	592	40,200	-	0.0341
244.1	13	596	40,600	-	0.0360
252	13	400	32,000	-	0.0221
260.1	13	600	52,200	-	0.0198
295	15	400	21,400	-	0.0179
302	15	401	10,900	-	0.0196
309	15	399	21,800	-	0.0171
321	15	395	32,800	-	0.0175
325	15	396	10,700	-	0.0193
417	29	400	33,200	-	0.0150
419	29	399	33,400	-	0.0152
445	30	398	33,100	-	0.0164
456	30	399	33,200	-	0.0165
457	30	399	33,200	-	0.0165
464	30	499	42,700	-	0.0157
476	30	503	43,500	465	0.0158
484	30	498	42,500	465	0.0163
485	30	400	33,400	465	0.0163
486	30	501	43,000	335	0.0157
496	30	501	43,000	335	0.0156
893	39	445	25,000	-	0.0179
900	39	445	25,600	-	0.0174
901	39	368	20,800	110	0.0178
902	39	370	20,500	110	0.0187
911	39	603	17,400	-	0.0157
920	39	604	17,600	-	0.0159
921	39	501	28,000	-	0.0177
931	39	502	28,400	-	0.0170
932	39	570	32,800	-	0.0163
942	39	569	33,200	-	0.0162
943	39	604	17,400	900	0.0160
951	39	604	17,200	900	0.0166

P.A.L.-P.J.B 4-16-51

FIG.25

COMPARISON OF UCLA ISOTHERMAL FRICTION FACTORS FOR WATER TEMPERATURES OF 400 TO 600 F WITH MOODY SMOOTH TUBE

- -TUBE 13 NO INSPECTION-NO PH CONTROL
- -TUBE 15 NO INSPECTION-NO PH CONTROL
- -TUBE 29 CLEAN SHINY
- -TUBE 30 VERY DIRTY BROWN BLACK } PH ≧ 9.5
- -TUBE 39 CLEAN STRAW COLORED

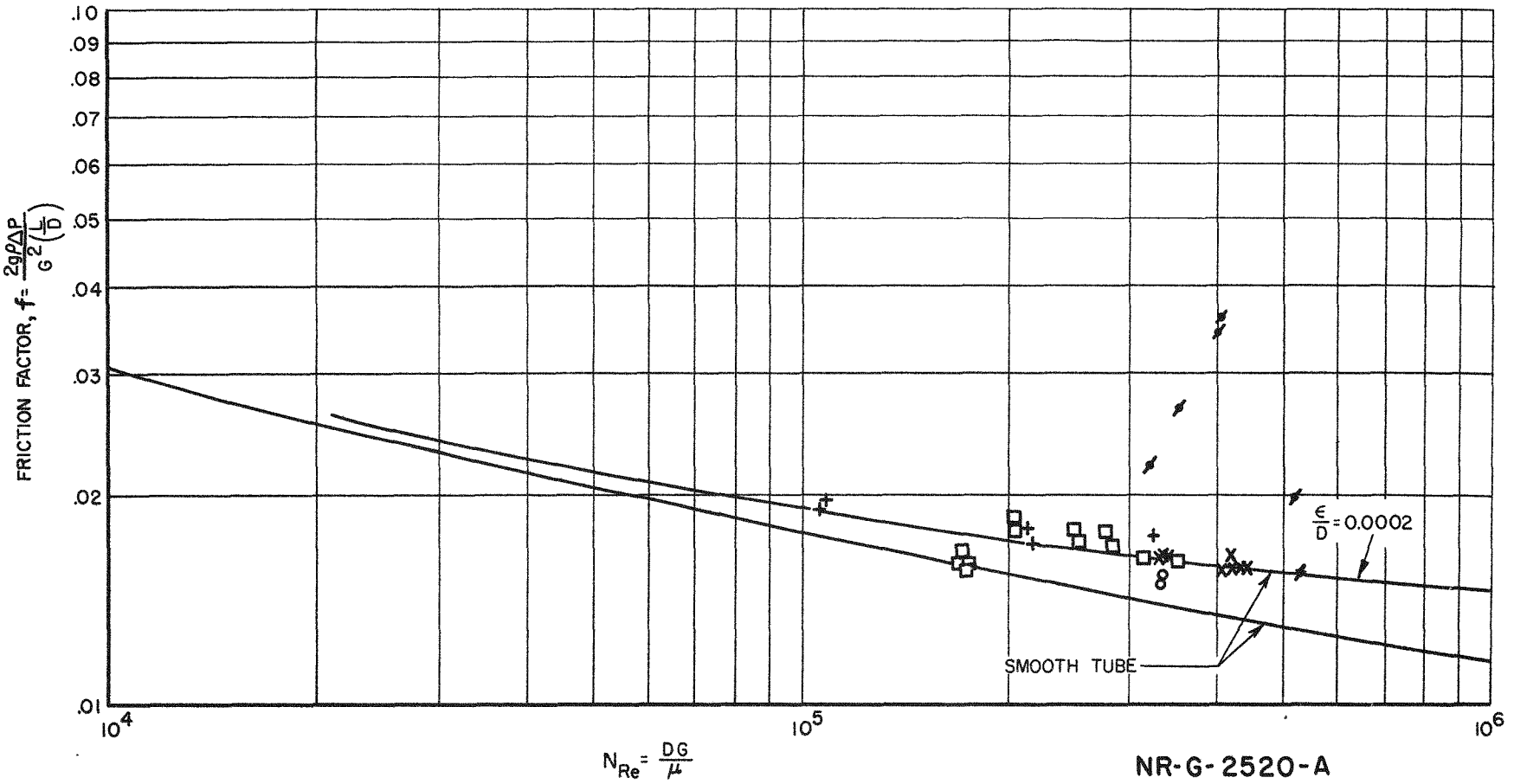

P.A.L.-P.J.B. 4-11-51

FIG. 26
COMPARISON OF PURDUE NON-ISOTHERMAL FRICTION FACTORS WITH THE MOODY SMOOTH TUBE (DATA CORRELATED BY PURDUE UNIVERSITY)

55

○ = ROUND TUBE
□ = SQUARE TUBE

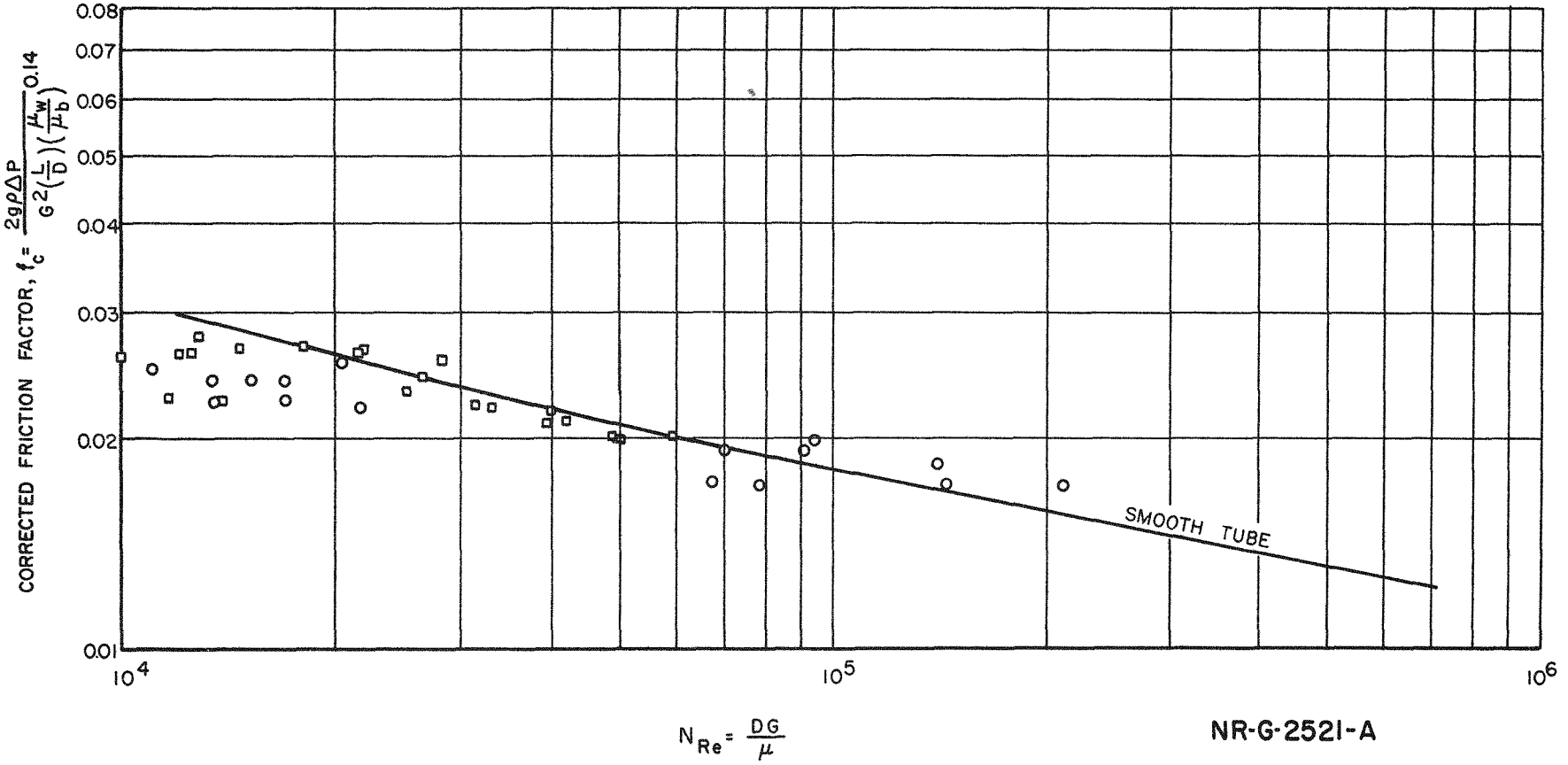

NR-G-2521-A

ES-895

P.A.L.-P.J.B.
4-17-51

FIG. 27
COMPARISON OF UCLA PRESSURE DROP DATA WITH BOILING, WITH CALCULATED PRESSURE DROP AT HIGH MASS FLOW RATE OF 7.65×10^6 LB/HR FT^2 AND INLET WATER TEMPERATURE AT 600 F AND PRESSURE AT 2000 PSIA

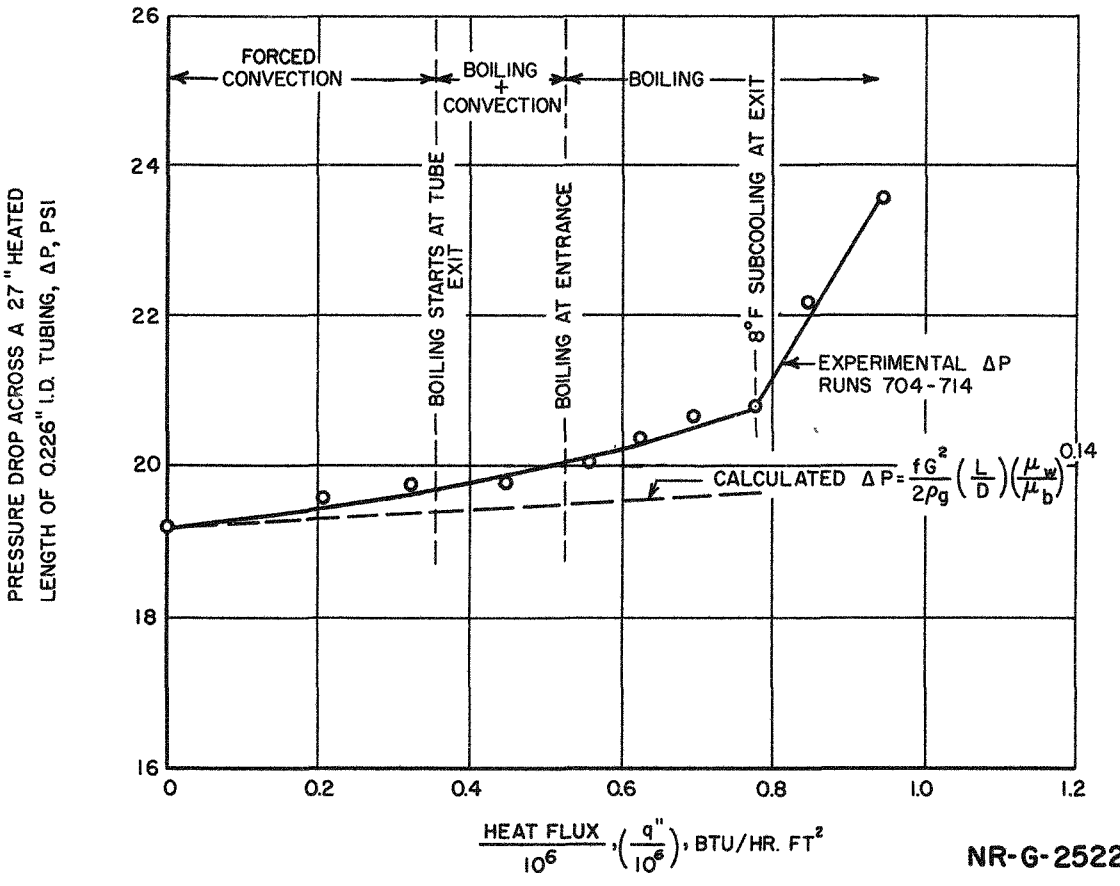

568-54

TABLE VII - UCLA BOILING AND NON-BOILING PRESSURE DROP DATA

Run No.	Exit Pressure, psia	Inlet Subcooling, F	Exit Subcooling, F*	Mass Flow Rate x 10^{-6} lb/hr ft^2	Nitrogen Content, cc/liter	$\frac{\Delta(\Delta P)^*}{\Delta P} \Big/ \frac{\Delta q''}{q''}$
583-597	2000	36	8	5.73	-	0.84
598-610	2000	36	8	5.73	710	0.77
696-703	2000	36	8	3.81	-	0.85
704-714	2000	36	8	7.65	-	0.60
911-920	2000	33	7	1.91	-	1.0
728-737	2000	35	11	7.65	710	0.58
943-951	2000	30	15	1.91	900	0.54
832-842	500	96	13	0.955	-	2.0
720-727	2000	36	17	3.81	770	0.39
860-866	100	98	18	3.81	-	7.2
619-625	250	100	15	3.81	-	8.2
611-618	100	100	23	3.81	-	7.4
843-859	500	93	25	7.65	-	0.87
820-831	500	96	28	3.81	-	2.3
642-648	1500	100	32	3.81	-	1.0
901-910	500	96	26	3.81	110	1.2
635-641	1000	100	27	3.81	-	2.0
476-485	2000	137	61	5.73	465	0.95
810-819	2000	133	62	7.65	-	0.34
464-474	2000	136	71	5.73	-	0.37
486-496	2000	136	71	5.73	335	0.37
511-522	2000	136	71	5.73	705	0.44
1008-1018	2000	133	70	7.65	-	0.28
877-888.1	500	236	98	3.81	-	7.4

* At conditions where pressure drop rapidly increases.

P.A.L.-P.J.B
4-10-51

FIG. 28
UCLA PRESSURE DROP DATA WITH BOILING: EFFECT OF DISSOLVED GAS ON PRESSURE DROP AT MASS FLOW RATE OF 1.91×10^6 POUNDS PER HR. SQ. FT. WITH INLET WATER TEMPERATURE AT 600F AND PRESSURE AT 2000 PSIA

58

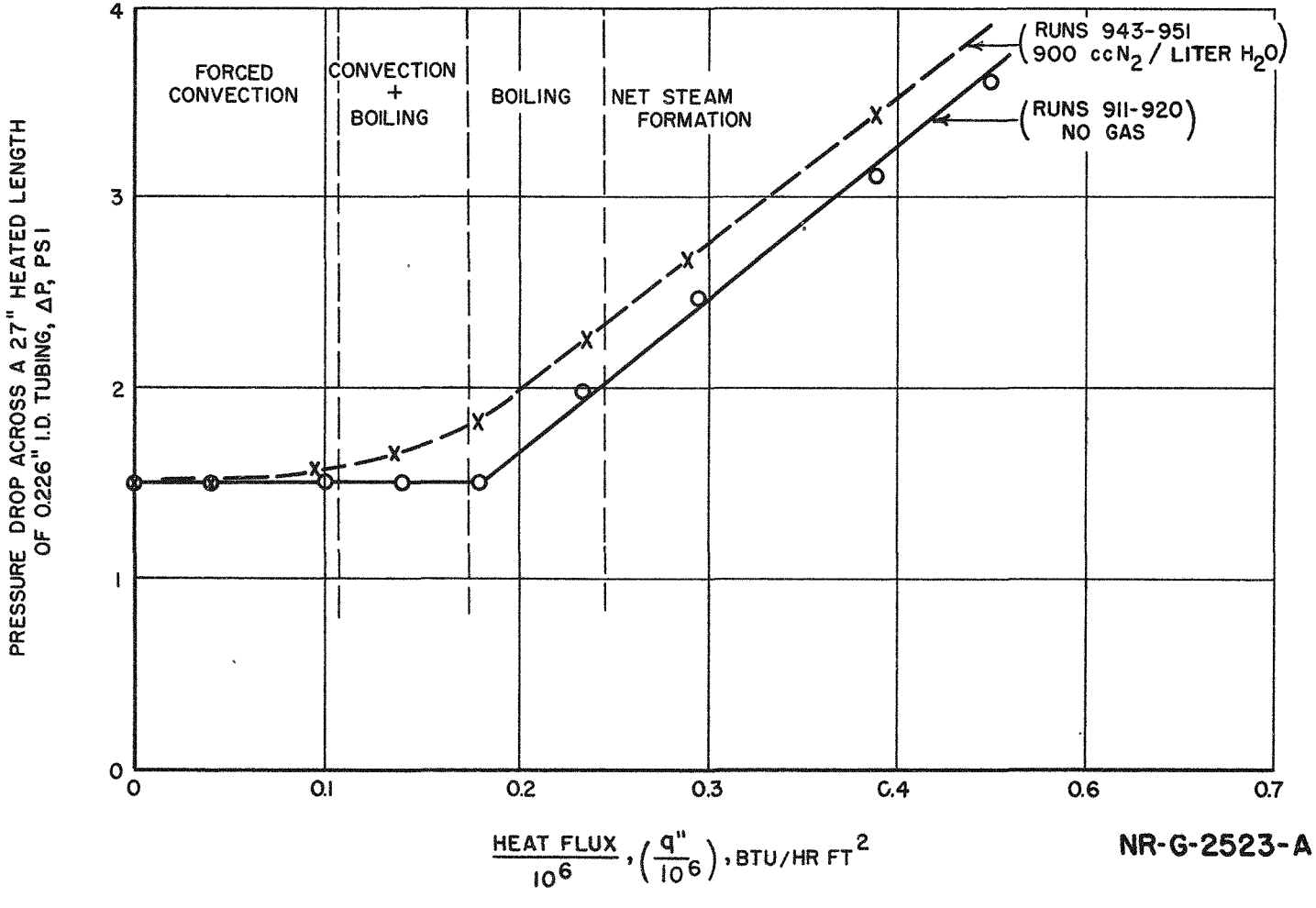

P.A.L., T.L., 4-16-51

FIG.29

UCLA PRESSURE DROP DATA WITH BOILING: EFFECT OF DISSOLVED GAS ON PRESSURE DROP AT MASS FLOW RATE OF 5.73×10^6 LB PER HR. SQ.FT. WITH INLET WATER TEMPERATURE AT 600 F AND PRESSURE AT 2000 PSIA

x RUNS 598-610, 710 cc N_2/LITER H_2O

o RUNS 583-597, NO GAS

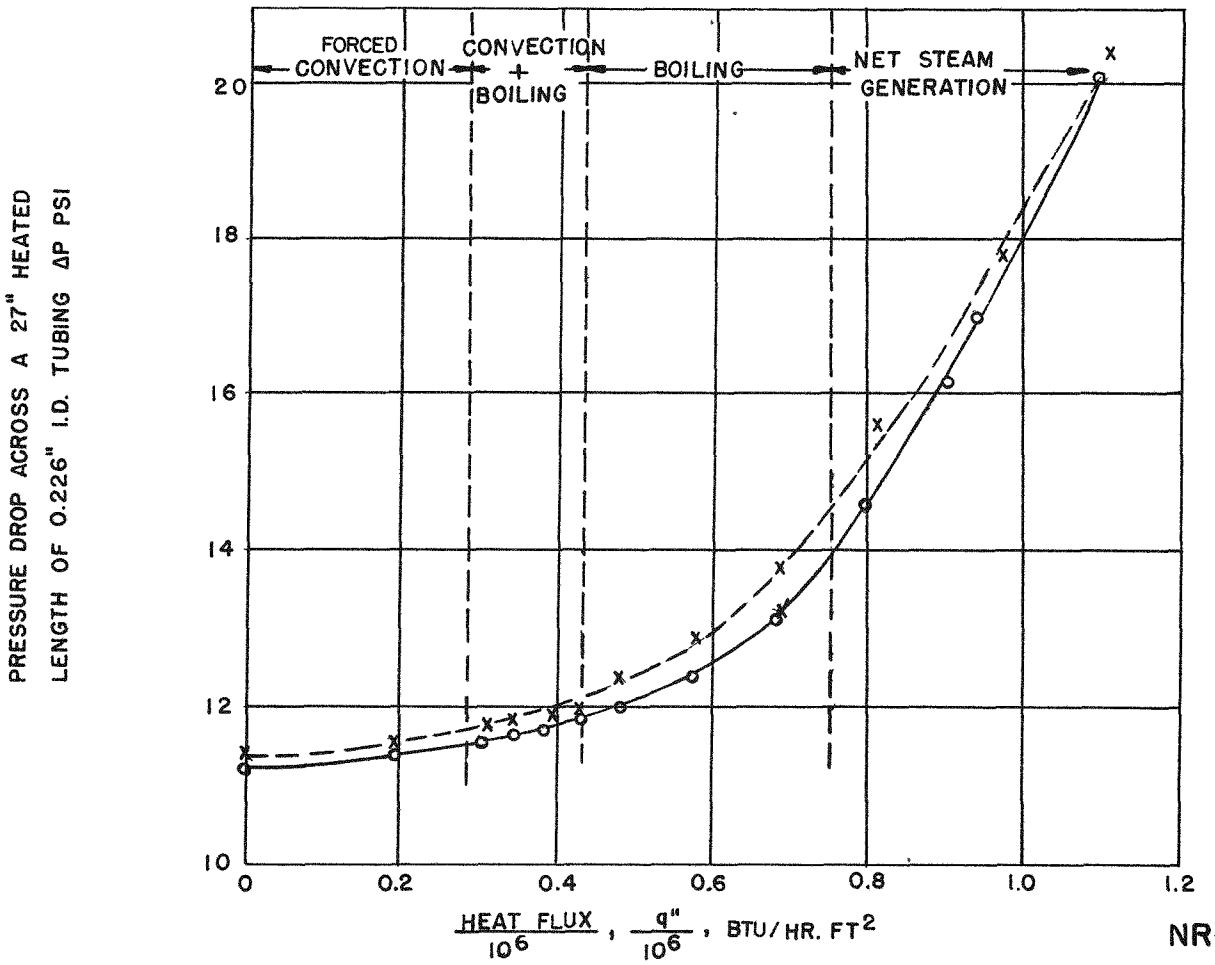

NR-G-2524-A

P.A.L., T.L., 4-16-51

FIG. 30

UCLA PRESSURE DROP DATA WITH BOILING: EFFECT OF DISSOLVED GAS ON PRESSURE DROP AT MASS FLOW RATE OF 7.65×10^6 LB. PER HR. SQ. FT. WITH INLET WATER TEMPERATURE AT 600 F AND PRESSURE AT 2000 PSIA

x RUNS 728-737, 710 cc N_2 / LITER H_2O

o RUNS 704-714, NO GAS

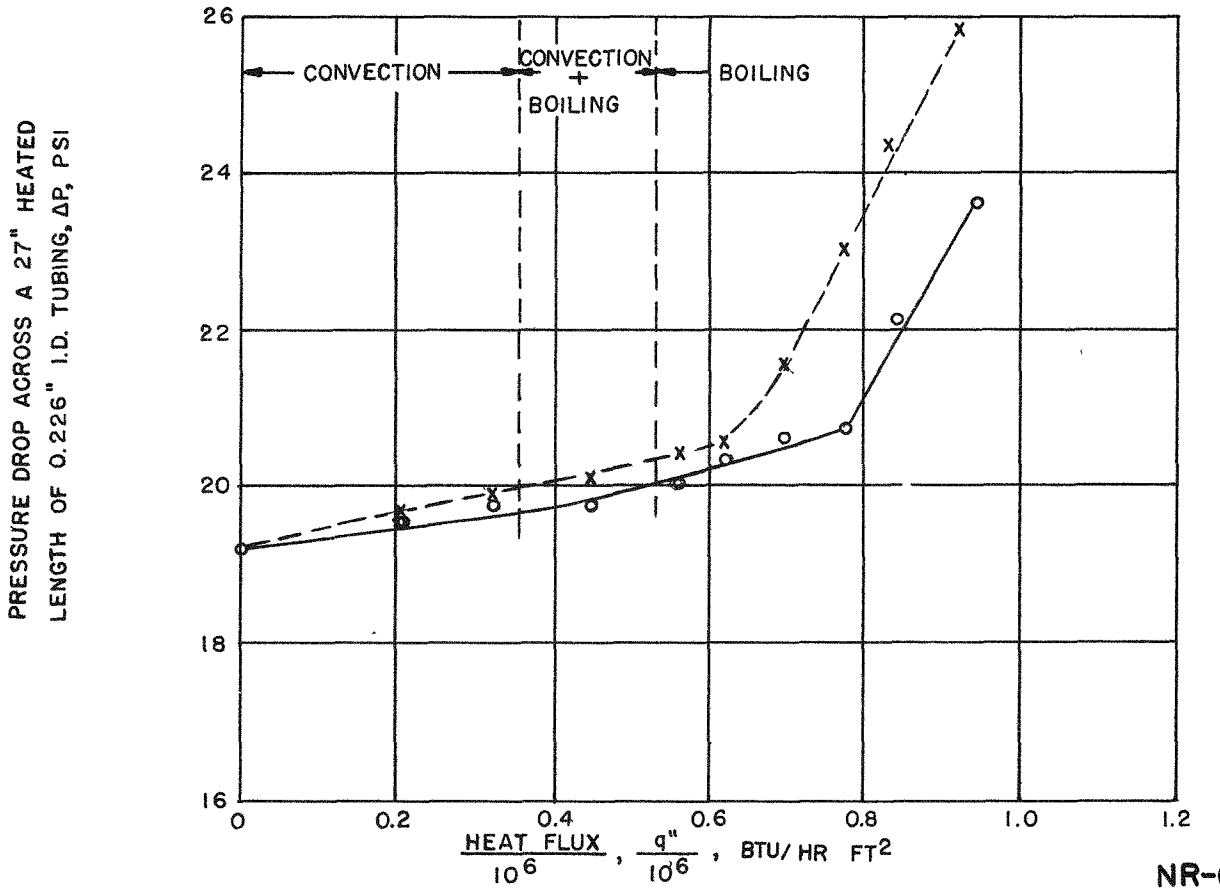

NR-G-2525-A

P.A.L.-P.J.B
4-20-51

FIG. 31
UCLA PRESSURE DROP DATA WITH BOILING - EFFECT OF DISSOLVED GAS ON PRESSURE DROP AT MASS FLOW RATE OF 5.73×10^6 LB / HR. SQ. FT. WITH INLET WATER TEMPERATURE AT 500F AND PRESSURE AT 2000 PSIA

O = RUNS 464-474, NO GAS
X = RUNS 511-522, 705 cc N_2 / LITER H_2O

61

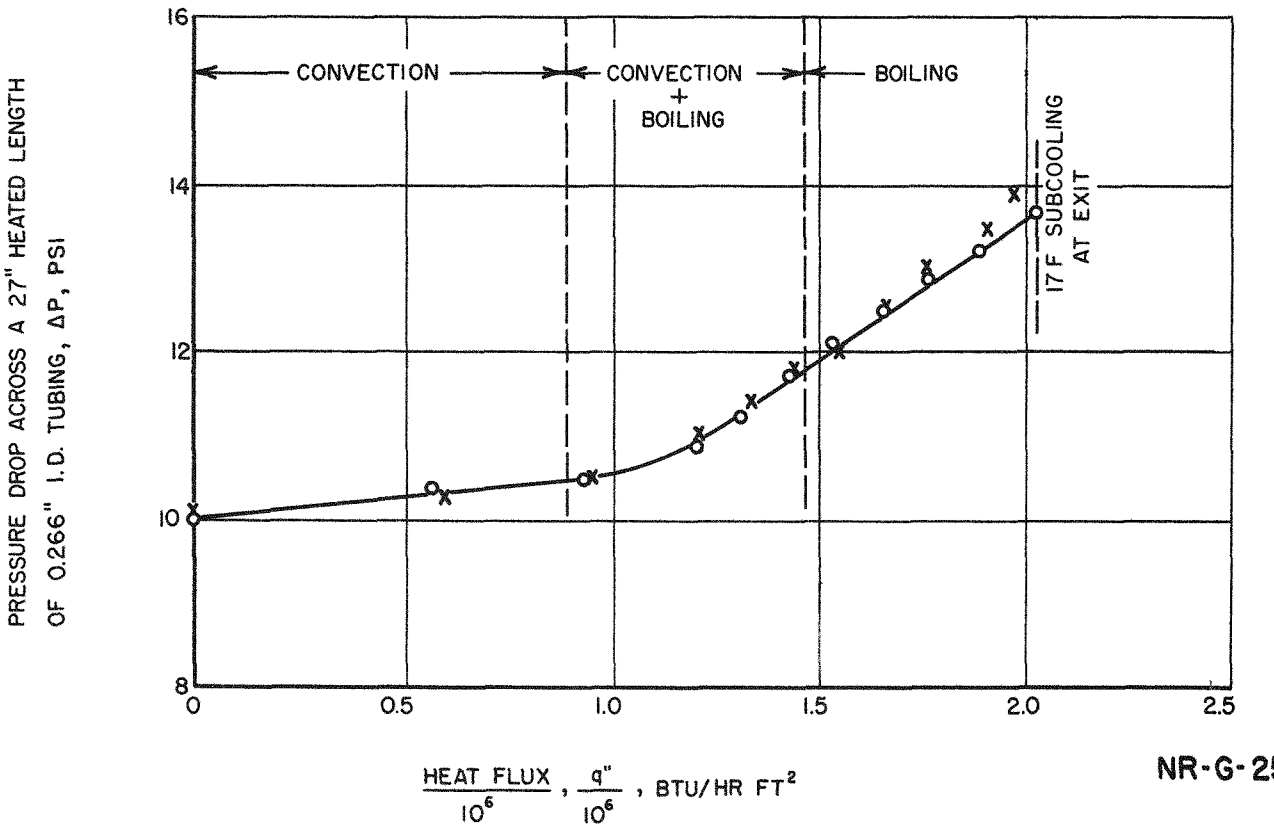

NR-G-2531-A

45-895

P.A.L-P.J.B.
4-20-51

FIG. 32

UCLA PRESSURE DROP DATA WITH BOILING: EFFECT OF DISSOLVED GAS ON PRESSURE DROP AT MASS FLOW RATE OF 1.93×10^6 LB / HR. SQ. FT. WITH INLET WATER TEMPERATURE AT 400F AND PRESSURE AT 2000 PSIA

O = RUNS 558-569, NO GAS

X = RUNS 570-581.1, 750 cc N_2 / LITER H_2O

62

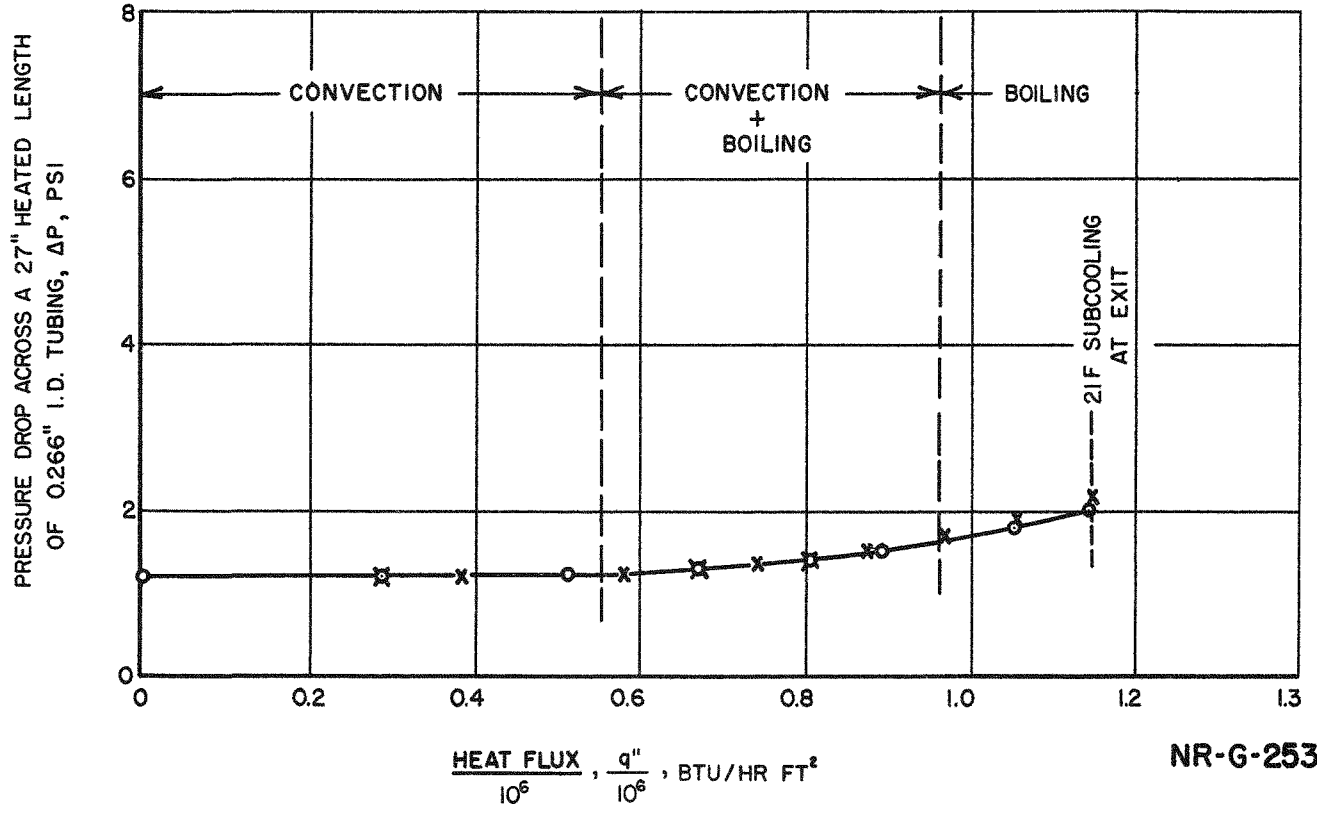

NR-G-2532-A

-P.J.B. 4-10-51

FIG. 33
EFFECT OF LOCAL BOILING AND WATER TEMPERATURE ON PRESSURE DROP (PURDUE UNIV.)

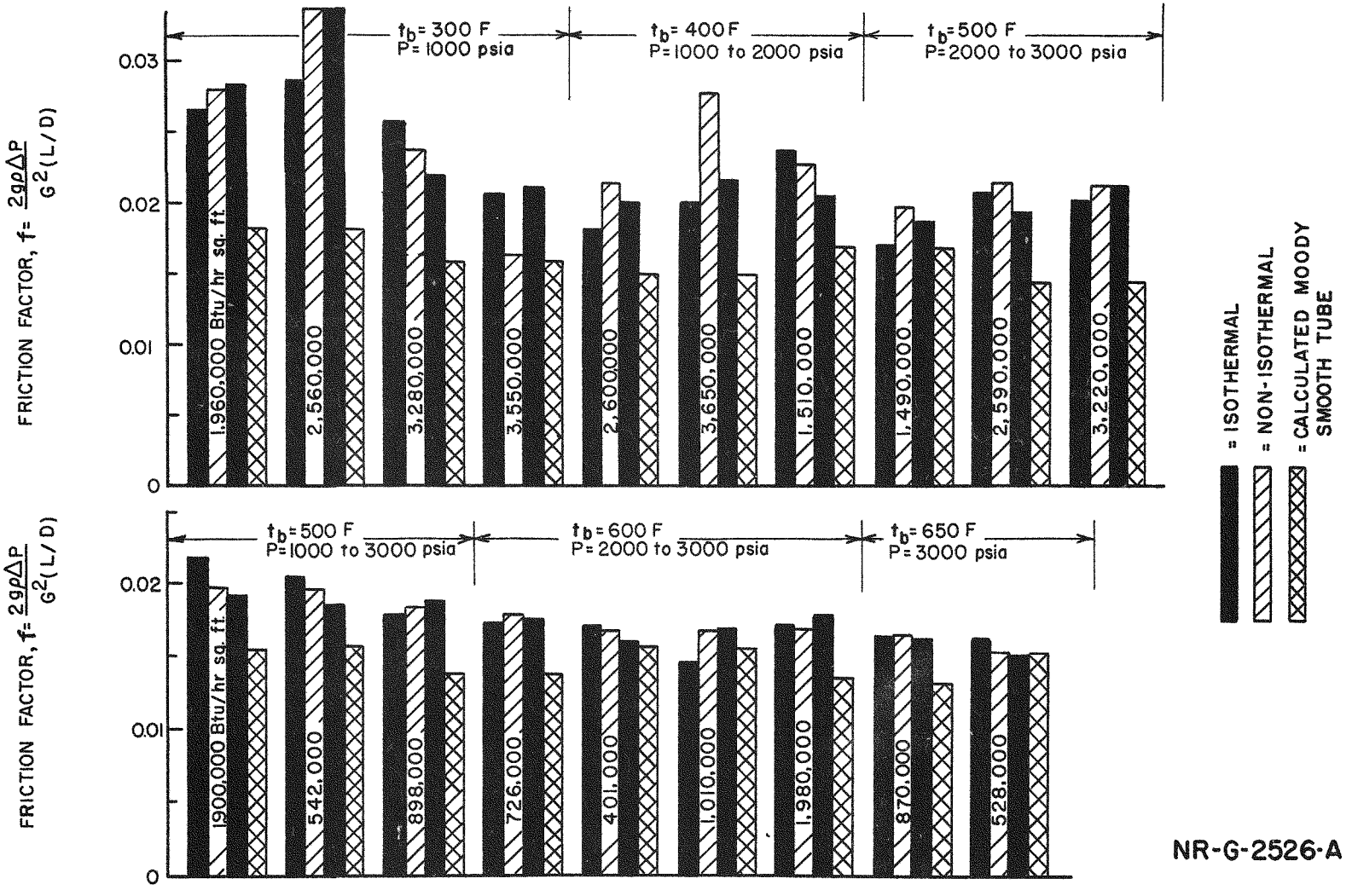

64

TABLE VIII - MIT BOILING AND NON-BOILING PRESSURE DROP DATA

Run No.	Pressure Drop Inch H_2O	Heat Flux x 10^{-6}, Btu/hr sq ft	Inlet Water Temperature, F	Outlet Water Temperature, F
		P = 2000 psia, V = 30 fps		
28-- 1	102	2.06	448	508
33--11	115	2.49	386	470
33--12	119	2.775	398	491
33--13	126	3.02	403	503
		P = 2000 psia, V = 20 fps		
30-- 1	53.6	0.811	373	414
30-- 2	52.9	1.180	409	467
30-- 3	56	1.806	436	523
30-- 4	63	2.07	440	539
30-- 5	65	2.265	428	537
30-- 6	65	2.05	424	523
31-- 1	57.2	0.629	327	358
31-- 2	55	0.840	350	391
31-- 3	54.3	0.961	382	429
31-- 4	52.2	1.188	408	466
31-- 5	53	1.532	431	504
31-- 6	57	1.758	435	519
31-- 7	62	1.921	421	514
31-- 8	62	2.085	420	520
31-- 9	62	2.325	340	454
31--10	62	2.550	340	464
		P = 2000 psia, V = 10 fps		
34-- 2	25	0.306	223	252
34-- 3	22.9	1.05	371	470
34-- 4	22.9	1.29	389	512
34-- 5	23	1.475	387	527
34-- 6	24	1.625	376	531
34-- 7	27	1.835	309	487
		P = 1500 psia, V = 30 fps		
32-- 1	116.5	0.409	305	318
32-- 2	114.2	0.592	314	333
32-- 3	110	0.739	348	373
32-- 4	106	0.992	379	412
		P = 1500 psia, V = 30 fps		
32-- 5	101.5	1.343	423	467
32-- 6	110	1.866	439	500
32-- 7	120	2.13	431	501
32-- 8	120	2.305	390	468
32-- 9	121	2.43	397	478
32--10	127	2.57	397	484
32--11	130	2.775	396	489
		P = 1500 psia, V = 20 fps		
33-- 2	56.5	0.705	323	357
33-- 3	52.2	1.033	376	427
33-- 4	60.0	1.415	430	499
33-- 5	66	1.630	425	504
33-- 6	72	1.830	426	515
33-- 7	76	1.925	422	517
33-- 8	78	2.085	426	527
33-- 9	86	2.32	427	539
33--10	89	2.585	413	534
		P = 1500 psia, V = 10 fps		
35-- 3	16.4	0.496	355	404
35-- 4	16.4	0.839	357	439
35-- 5	19.5	1.137	376	487
35-- 6	24.5	1.392	396	528
35-- 7	25.5	1.563	385	534
35-- 8	26.5	1.810	309	485
35-- 9	27.5	1.846	319	499

W.H.J.-P.J.B. 4-11-51

65

FIG.34
COMPARISON OF MIT NON-ISOTHERMAL FRICTION FACTORS WITH THE MOODY SMOOTH TUBE

NON-BOILING FORCED CONVECTION
TEST DATA, P=2000 & 1500 PSIA

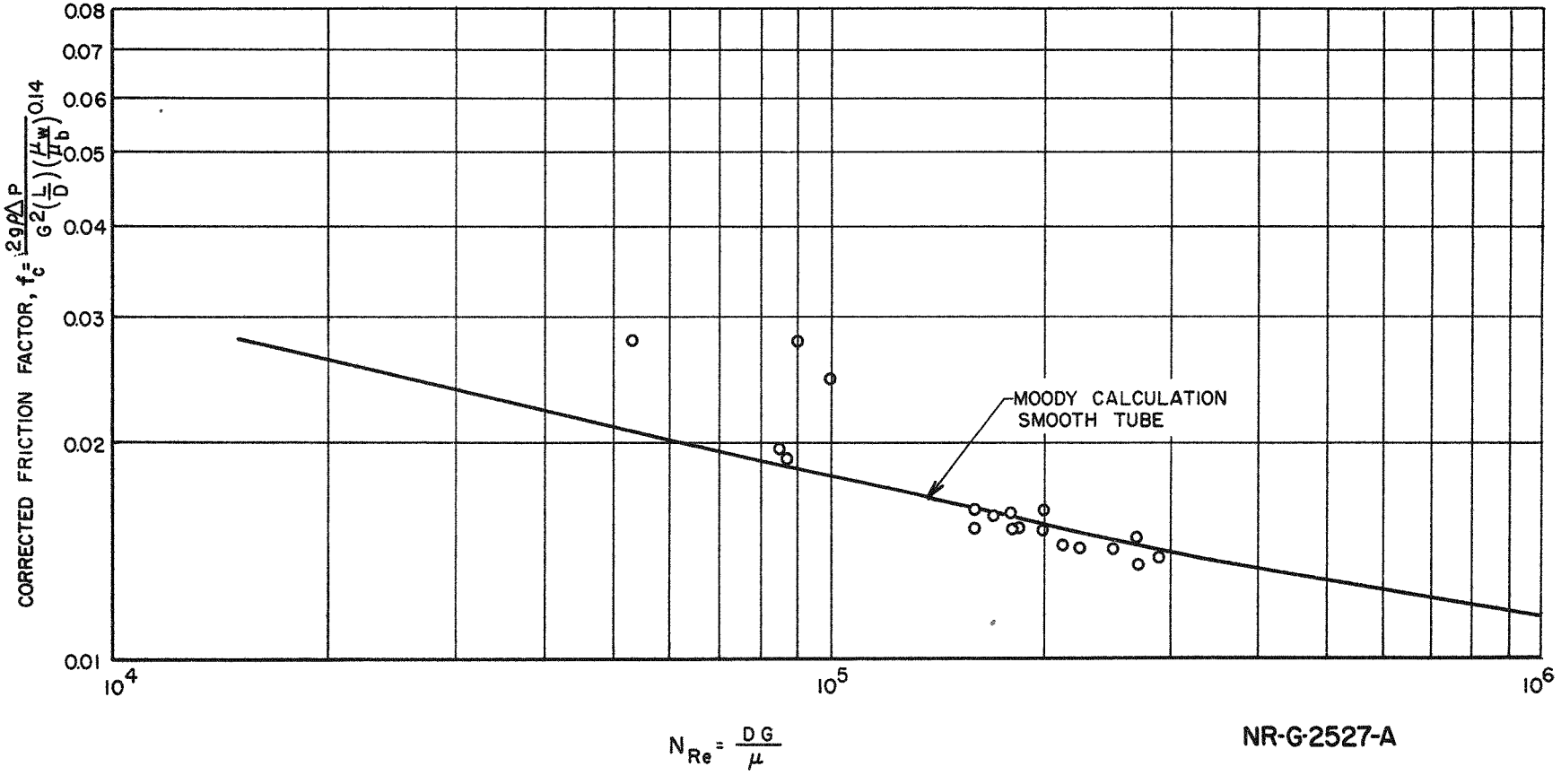

TABLE IX - UCLA DENSITY DATA WITH AND WITHOUT LOCAL BOILING

Pressure, psia	Heat Flux x 10^{-6} Btu/hr ft^2	Calculated Temperature of Subcooling, F*	Per cent Density Change
500	0.20	20	+ 3.17
500	0.40	20	+ 0.57
500	0.60	18	- 1.59
500	1.01	16	- 1.97
500	1.23	13	-10.8
500	1.42	12	-35.9
500	1.61	10	-44.6
500	0.19	16	- 0.5
500	0.42	17	- 1.0
500	0.62	16	+ 1.02
500	0.82	19.5	- 5.4
500	1.04	18.5	-11.3
500	1.19	24	- 4.2
500	1.44	6	-28.5
1000	0.2	17	- 1.47
1000	0.42	17	- 0.21
1000	0.61	14	- 0.85
1000	1.02	9.5	-12.55
1000	1.23	5.5	-16.4
1000	1.42	4.5	-20.3
1000	1.51	1.0	-19.0
1000	0.86	20.5	+ 1.74
1000	1.26	16	-12.7
1000	1.41	21	-29.4
1000	1.01	20.5	-16.7
1000	0.60	22	- 6.71
2000	0.16	36	0
2000	0.62	36	- 3.8
2000	1.01	36	- 0.7
2000	1.58	36	+ 0.1
2000	0.23	16	0
2000	0.42	16	+ 0.3
2000	0.62	16	- 1.5
2000	0.75	16	- 0.9
2000	0.91	16	0
2000	1.09	16	- 3.0
2000	0.24	84	+ 0.4
2000	0.24	84	+ 0.4
2000	0.45	84	+ 0.3
2000	0.78	84	+ 0.3
2000	0.78	84	+ 0.9
2000	1.03	84	+ 0.1
2000	1.04	84	- 0.3
2000	1.42	84	0
2000	1.47	84	0

* The values of subcooling pressures of 2000 psia were only approximate since the exact data are not available.

W.H.J.-P.J.B. 4-12-51

FIG.35
EFFECT OF HEAT FLUX AND WATER TEMPERATURE ON WATER DENSITY AT 2000 PSIA AND MASS FLOW RATE OF 3.75 X 10^6 LB PER HR. SQ.FT. (UCLA)

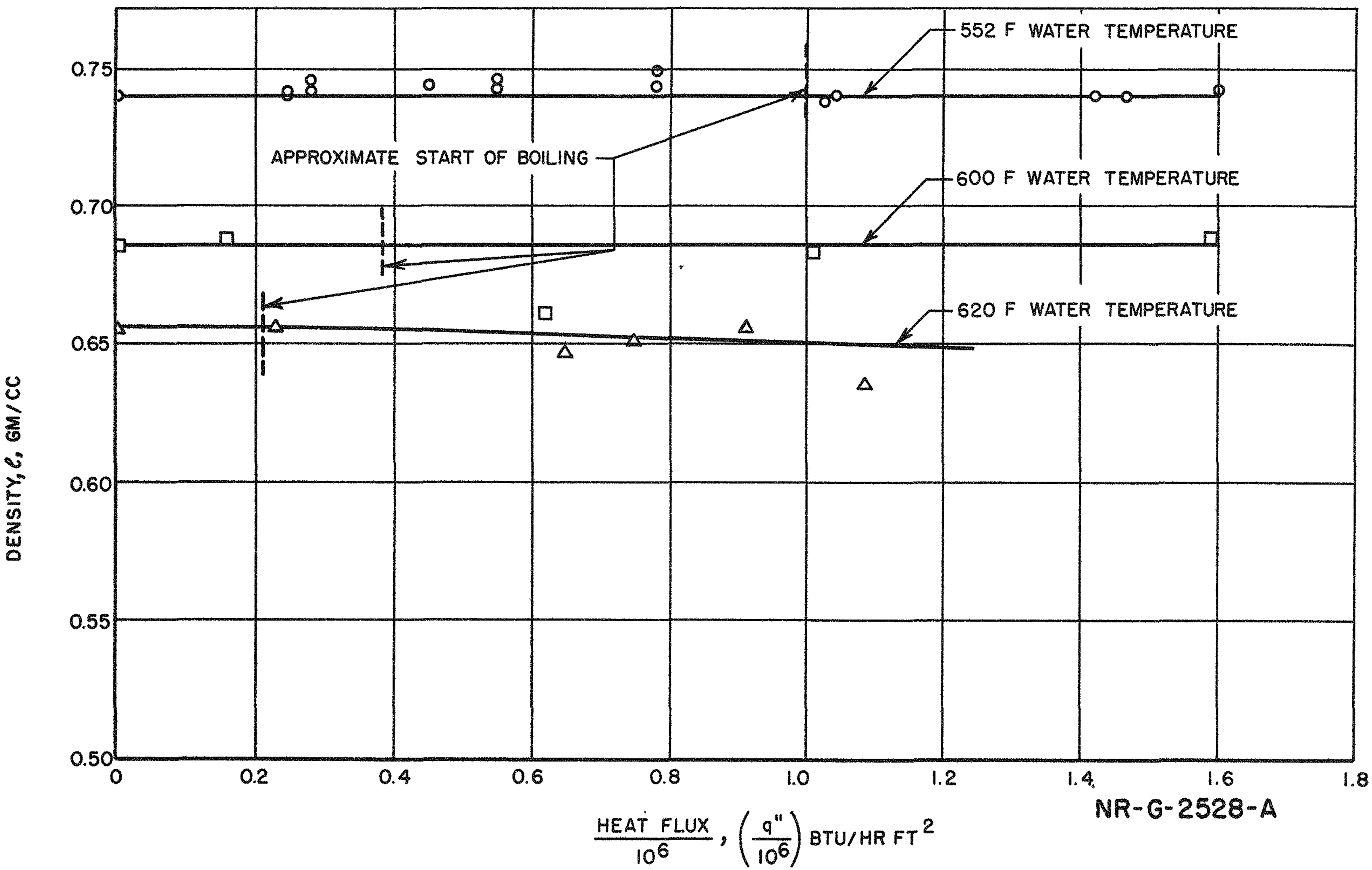

NR-G-2528-A

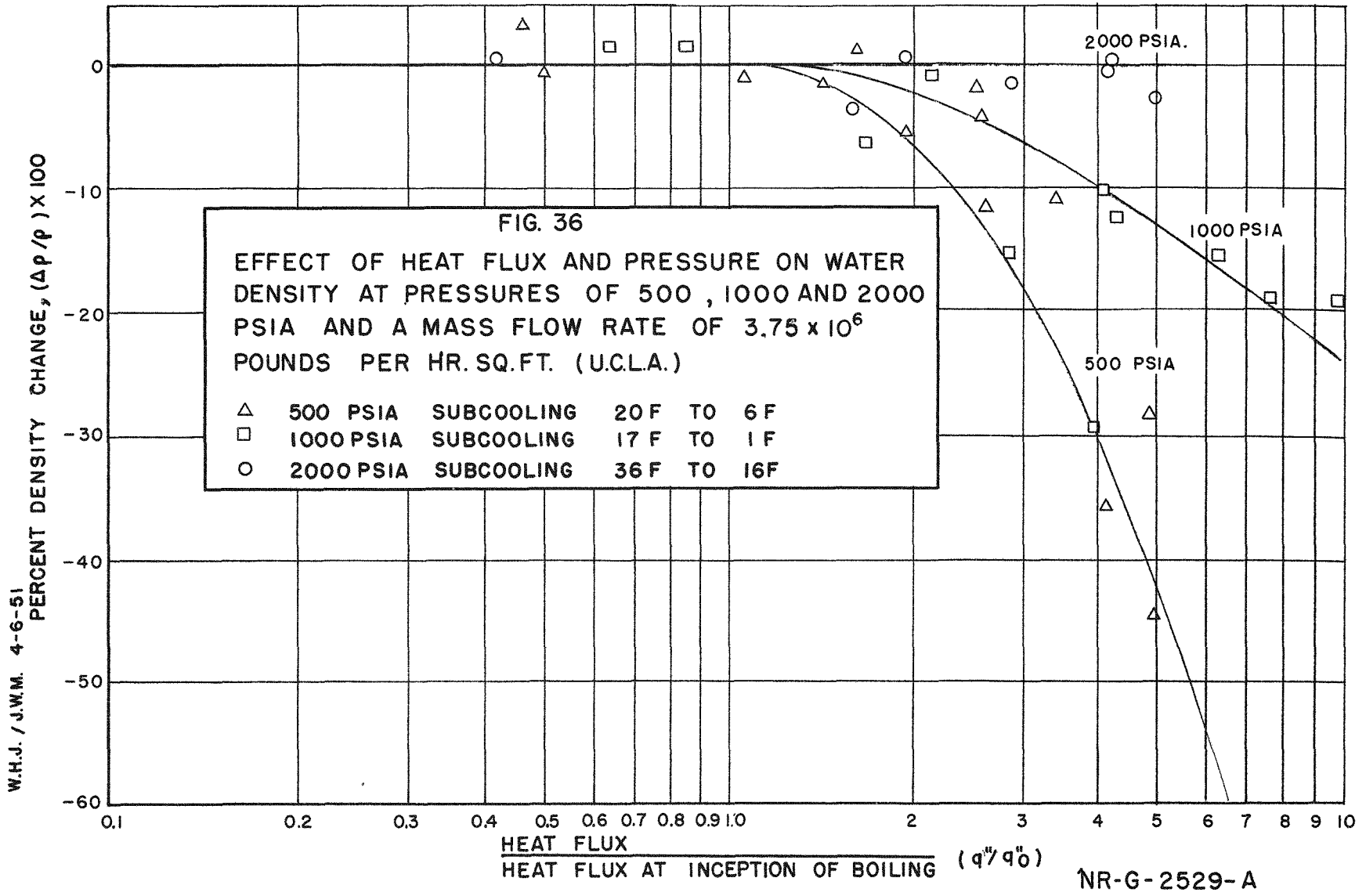

FIG. 36

EFFECT OF HEAT FLUX AND PRESSURE ON WATER DENSITY AT PRESSURES OF 500 , 1000 AND 2000 PSIA AND A MASS FLOW RATE OF 3.75×10^6 POUNDS PER HR. SQ.FT. (U.C.L.A.)

△	500 PSIA	SUBCOOLING	20 F	TO	6 F
□	1000 PSIA	SUBCOOLING	17 F	TO	1 F
○	2000 PSIA	SUBCOOLING	36 F	TO	16F

B. Development of Density Equation

In F. C. Gunther's paper (2) on bubble studies, the following nomenclature was used.

R_{max} = radius at full growth of the "average" bubble at the heat transfer condition

θ = lifetime of an "average" bubble associated with the heat transfer condition, sec.

N = number of new bubbles of average size appearing on a unit area per unit time .

t = time, sec.

According to Gunther the bubbles grow into hemispheres which slide along the surface of the heater strip in the direction of water flow but never leave the surface. Data were reported for the average surface area covered by one average bubble. This was shown by Gunther to be

$$A = \frac{1}{\theta}\int_0^{\theta} \pi R^2(t)dt = 0.57\pi R^2_{max}$$

The total volume of one hemispherical bubble as found from the above equation and the standard formulas for the cross sectional area and volume of a sphere is,

$$V = 0.9\ R^3_{max}$$

The total volume occupied by bubbles for each square inch of surface area is

$$V_b = 0.9\ R^3_{max}\ \theta N$$

The density of a mixture of vapor bubbles and liquid is

$$\rho_{mix} = \frac{\rho_\ell (V_{mix} - V_b) + V_b \rho_V}{V_{mix}} = \rho_\ell - \frac{V_b}{V_{mix}}(\rho_\ell - \rho_V)$$

$$\frac{\rho_{mix}}{\rho_\ell} = 1 - \frac{V_b}{V_{mix}}\frac{(\rho_\ell - \rho_V)}{\rho_\ell}$$

where ρ_{mix} = density of mixture of vapor bubbles and liquid

ρ_V = density of vapor

ρ_ℓ = density of liquid

V_{mix} = volume of mixture

V_b = volume of vapor

The per cent density change from a condition of no boiling to a condition of boiling is

$$\delta = 100\left(\frac{\bar{\Delta\rho}}{\rho_l}\right) = 100\left(\frac{\rho_l - \rho_{mix}}{\rho_l}\right)$$

Therefore

$$\delta = 100\left(\frac{V_b}{V_{mix}}\right)\left(1 - \frac{\rho_V}{\rho_{mix}}\right)$$

In the calculations, ρ_V was considered zero, giving the largest possible value for δ in the above equation and simplifying the equation to

$$\delta = 100\left(\frac{V_b}{V_{mix}}\right)$$

Combining this equation with the relation for the volume of the bubbles,

$$\delta = \frac{90\ R_{max}^3\ \theta N}{V_{mix}}$$

Consider the condition of surface boiling from both sides of a parallel plate channel with 1/8 in. between the plates. The volume of the mixture between the plates per square inch of plate area is

$$V_{mix} = 1 \text{ in.} \times 1 \text{ in.} \times 1/8 \text{ in.} = 1/8 \text{ cu in.}$$

Applying a factor of two to allow for heating from both sides of the channel and a factor of two to account for the possibility of spherical bubbles instead of hemispherical bubbles, the equation for density changes in a 1/8 inch channel becomes

$$\delta = 2880\ R_{max}^3\ \theta N$$

By applying Gunther's data to this equation, the following equation was found:

$$\delta = \frac{\Delta\rho}{\rho} \times 100 = \frac{3 \times 10^8\ (q''/q''_o)^{1.5}}{V\Delta T_{sub}^4}$$

The formula correlates the calculated and actual density changes by a factor of 2.5.

This equation applies to density changes of water flowing through the 1/8 inch rectangular channel at approximately one atmosphere pressure, 60 to 155F subcooling, 5 to 20 fps velocity, and 726,000 to 3,370,000 Btu per hr sq ft heat flux The equation, when applied to the UCLA data for pressures of 500, 1000, and 2000 psia, shows that pressure has a large effect on density changes during local boiling. The UCLA data indicate much smaller density changes for the same condition of velocity, subcooling, and heat flux than the value given by the derived equation.

C. BIBLIOGRAPHY

1 Boelter, L. M K., and Staff.
Boiling Studies, AEC Research Contract No. AT-11-1-Gen-9.
Progress Report No. 1, August, 1949.

2. Gunther, F. C.
Boiling Heat Transfer to Water with Forced Convection, ASME Trans
Vol. 73, No. 2, February, 1951.

3. McAdams, W. H.
Heat Transmission, McGraw-Hill, New York, 1942

4. McAdams, W. H., J. N. Addoms, and W. E. Kennel
Heat Transfer at High Rates to Water with Surface Boiling, report
reproduced by Argonne National Laboratory, ANL-4268, December,
1948.

5. Moody, L. F.
Friction Factors for Pipe Flow, Trans ASME, Vol. 66, 1944, pp. 672-673

6. Weatherhead, R.
Thesis in Mechanical Engineering, Purdue University, 1950.